UNITED STATES DEPARTMENT OF THE INTERIOR

GEOLOGICAL SURVEY

PROBABILITIES OF LARGE EARTHQUAKES OCCURRING IN CALIFORNIA ON THE SAN ANDREAS FAULT

by

The Working Group on California Earthquake Probabilities

Open-File Report 88-398

This report is preliminary and has not been reviewed for conformity with U.S. Geological Survey editorial standards and stratigraphic nomenclature. Any use of trade names is for descriptive purposes only and does not imply endorsement by the USGS.

MENLO PARK, CALIFORNIA

1988

PREFACE

In late 1984, the National Earthquake Prediction Evaluation Council (NEPEC) agreed to meet several times per year to systematically review and synthesize data from areas in the United States considered to be most critical from an earthquake prediction standpoint. On May 9, 1986, NEPEC informed the Director of the U.S. Geological Survey that, as a result of several review meetings devoted to California and Alaska, it had identified 13 subareas on the San Andreas, San Jacinto and Hayward faults of California and two areas in Alaska for which opportunities existed to make significant progress in earthquake prediction during the next decade. Lynn R. Sykes, the chairman of NEPEC, briefed the subcommittee on earthquake studies that is advisory to the USGS and Frank Press, the President of the U.S. National Academy of Sciences, on those findings.

It was suggested as a further step that NEPEC review a published statement from the early 1980's that there was a 50 percent chance of a large and damaging earthquake in southern California during the subsequent 30 years. However, because that statement was not well-documented and new data on prehistoric earthquakes and slip-rates are now available for several places in California, Sykes recommended to the USGS that a working group be constituted to review the likelihood of a large earthquake in southern California. On March 30, 1987, Dallas L. Peck, the Director of USGS, wrote to NEPEC specifically charging it to evaluate the earthquake threat to southern California and to assess the likelihood of a great earthquake in southern California during the next few decades. At its meeting on April 2, 1987, NEPEC recommended that such a working group be constituted and report its findings to NEPEC. Because there also was a concern about the Hayward fault on the east side of San Francisco Bay, the working group was charged with evaluating the earthquake threat to the greater San Francisco Bay area as well.

A draft of this report of the Working Group on California Earthquake Probabilities was approved in principle by NEPEC on February 2, 1988, and was revised following suggestions made at that meeting. As new data are continually being gathered relevant to long-term forecasts for specific segments of major faults in California, it is expected that the conclusions of this document will need to be revised and updated every few years.

ACKNOWLEDGMENTS

The report was improved considerably by the thorough and careful editing of Janet L. Cluff. Thelma Rodriguez, Nancy Arp and Beverly Monroe provided assistance in helping with arrangements for the meetings of the Working Group and in preparing the report. Ray Buland is thanked for conversations and advice on method of the probability calculations. William Bakun provided technical review of the manuscript.

TABLE OF CONTENTS

EXECUTIVE SUMMARY

Because of increased public interest and concern about expected losses from future earthquakes in California, the National Earthquake Prediction Evaluation Council recommended that the probability of occurrence of large (magnitude 7 or greater) earthquakes in California be evaluated. In response to this recommendation, the U.S. Geological Survey formed the Working Group on California Earthquake Probabilities.

The Working Group met several times during the summer and fall of 1987 and winter of 1988 to review and assess the state of knowledge that would allow calculation of earthquake probabilities on specific fault segments. The scope of the evaluation was limited to assessing the probabilities for large earthquakes resulting from slip on the major faults of the San Andreas fault system. The evaluations were based on a probability model that assumes increase of probability with elapsed time since the previous major earthquake on the fault segment. To determine time-dependent probabilities, the faults were divided into their recognizable segments, and the potential for a future large earthquake on that segment was calculated based on the time that has elapsed since the most recent large earthquake, and fault parameters such as slip rate and amount of displacement.

Although there are numerous other active faults in California, almost all capable of moderate earthquakes between magnitudes 6 and 7 and some capable of producing large earthquakes, the Working Group concluded that, at this time, there are insufficient data for application of the methods of time-dependent probability calculations for these faults. Estimating future earthquake occurrence for the other recognized active faults is best approached by long-term seismic potential models that do not take into account the length of time since the previous earthquake and assume the hazard remains constant with time. Individually, these faults present a lesser threat than do the major faults of the San Andreas system, because their long-term slip rates, historical rates of earthquake occurrence, and size of earthquakes are less than those for the San Andreas. However, because these faults are not considered in our analysis, the probabilities computed for each region of California should be considered minimum values.

A report by the Federal Emergency Management Agency [*FEMA*, 1980] stated that a major earthquake in southern California, comparable to the great earthquake of 1857, has a probability greater than 0.5 in the next 30 years. The Working Group found that the earthquake hazard on the southern San Andreas fault is at least as high as that reported by *FEMA*. In addition, the Working Group concluded that somewhat smaller events, of magnitude 7 to $7\frac{1}{2}$, are of concern in southern California and in the San Francisco Bay area. Such events occurring near population centers could pose severe hazards, as discussed in the *FEMA* report.

The time interval chosen for the probability calculations was 30 years, 1988 to 2018, although similar calculations using the same models were performed for 5-year, 10-year, and 20-year intervals, as well. To distinguish fault segment models based on relatively good data from those based on poor or incomplete data, each segment was given a level of reliability rating from A to E, with A being most reliable.

The results of the Working Group's evaluations, judgments, analyses, and assessments are summarized on the following figure.

Within a region containing more than one fault segment, the total probability of the occurrence of at least one large earthquake is, for many applications, of greater interest than the probabilities for individual segments. The results of aggregating the individual probability values to forecast the probability of a large earthquake in three regions is summarized on the following table.

Probability of One or More Large Earthquakes on Faults of the San Andreas Fault System

Geographic Region or Fault	Expected Magnitude	Probability for Intervals Beginning 1/1/88			
		5 yr	10 yr	20 yr	30 yr
San Francisco Bay Area	7	0.1	0.2	0.3	0.5
Southern San Andreas Fault	7 1/2–8	0.1	0.2	0.4	0.6
San Jacinto Fault	6 1/2–7	0.1	0.2	0.3	0.5

- The 30-year probability of large earthquakes is highest in southern California. We have identified the 100-km-long Coachella Valley segment as having the highest probability (0.4) of producing an earthquake of magnitude 7 1/2 in the next 30 years. A major earthquake has not occurred there since about AD 1680. The Mojave segment, part of the source region of the great 1857 earthquake, has a 30-year probability of 0.3.

- Evaluation of the southern San Andreas fault depends critically on the future behavior of the San Bernardino Mountains segment. If the San Bernardino Mountains segment slips independent of the adjacent segments, the expected magnitude of earthquakes on the southern San Andreas fault would be about 7 1/2, with a total probability of at least one such event in the next 30 years of 0.7. If the San Bernardino Mountains segment slips along with either the Mojave segment to the north or the Coachella Valley segment to the south, then the resulting earthquake would approach the size of the 1857 earthquake, and have a 30-year probability of 0.6.

- The probability of large earthquakes within the next 30 years along fault segments in the San Francisco Bay Area is also significant. The total probability for all fault segments evaluated is 0.5. The Hayward fault has produced two earthquakes in historical time, in 1836 and 1868; both had estimated magnitudes approaching 7. The Northern East Bay segment of the Hayward fault, the Southern East Bay segment of the Hayward fault, and

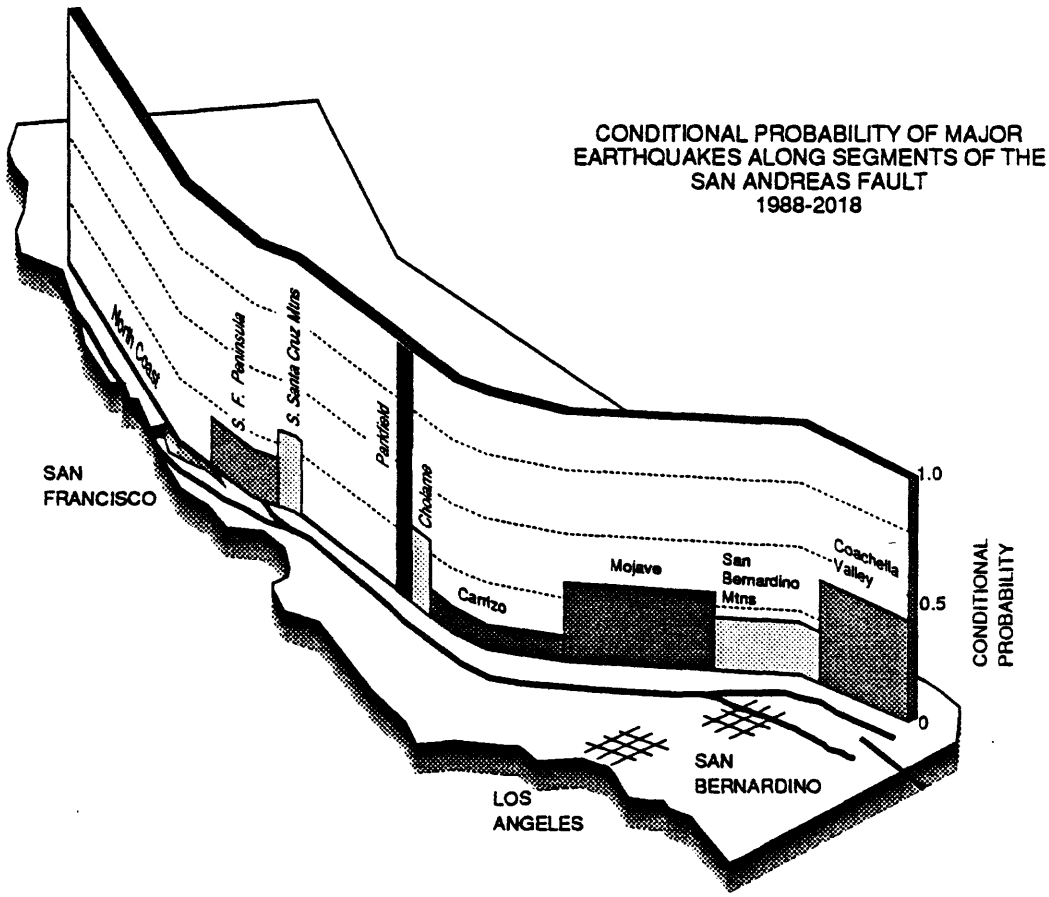
CONDITIONAL PROBABILITY OF MAJOR
EARTHQUAKES ALONG SEGMENTS OF THE
SAN ANDREAS FAULT
1988-2018
North Coast
S. F. Peninsula
S. Santa Cruz Mtns
Parkfield
Cholame
Carrizo
Mojave
San Bernardino Mtns
Coachella Valley
SAN FRANCISCO
LOS ANGELES
SAN BERNARDINO
1.0
0.5
0
CONDITIONAL PROBABILITY

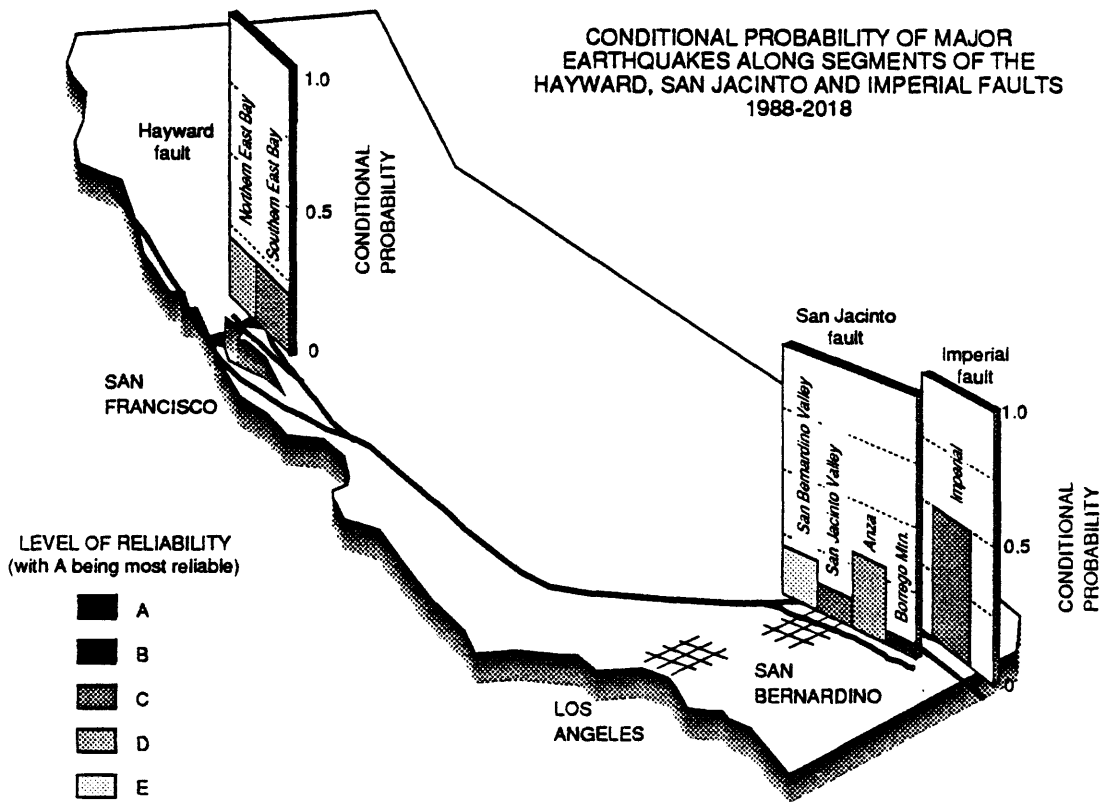
CONDITIONAL PROBABILITY OF MAJOR
EARTHQUAKES ALONG SEGMENTS OF THE
HAYWARD, SAN JACINTO AND IMPERIAL FAULTS
1988-2018
Hayward fault
Northern East Bay
Southern East Bay
San Jacinto fault
Imperial fault
San Bernardino Valley
San Jacinto Valley
Anza
Borrego Mtn.
Imperial
SAN FRANCISCO
LOS ANGELES
SAN BERNARDINO
1.0
0.5
0
CONDITIONAL PROBABILITY
LEVEL OF RELIABILITY
(with A being most reliable)
A
B
C
D
E

the San Francisco Peninsula segment of the San Andreas fault each have a probability of 0.2 of an earthquake of magnitude 7 in the next 30 years. The 30-year probability of a great earthquake along the North Coast segment, extending north from the San Francisco Peninsula, is less than 0.1.

- Fewer data are available about the recurrence of large earthquakes along five separate segments of the San Jacinto fault. During the course of the Working Group's deliberations, the magnitude 6.6 1987 Superstition Hills earthquake occurred on one of these segments. The Working Group estimated a probability of 0.5 for the four remaining segments combined, for the occurrence of earthquakes of about magnitude 7 within the next 30 years. The segment of the San Jacinto fault having the highest probability is the Anza segment (0.3). The others are: San Bernardino Valley segment, 0.2; San Jacinto Valley segment, 0.1; and the Borrego Mountain segment, less than 0.1.

The assessment of long-term seismic hazard on California's major faults is an active and rapidly developing field. New data and improvements in the model on which the assessments are based will probably lead to revision and refinement in the probabilities assigned here to segments of the San Andreas system. In addition, alternate interpretations of fault segmentation may also lead to somewhat different probabilities at specific locations. However, the total regional values are much less sensitive to the detailed recurrence characteristics of individual segments. These cumulative values are quite robust and support the main conclusion of our study, that the probability of a major earthquake on the San Andreas in southern California within the next 30 years is high, about 0.6; this probability approaches 0.5 both in the San Francisco Bay Area, and along the San Jacinto fault.

INTRODUCTION

In the 175-year period from 1812 to 1987, California experienced at least 11 large earthquakes of about magnitude 7 or greater. Two of these events were the great earthquakes of 1857 and 1906, in which the San Andreas fault ruptured, affecting the areas of Los Angeles and San Francisco, respectively. Similar earthquakes will certainly occur in the future and can be expected to have significant impact on California and the Nation. Property losses resulting from a repeat of the 1857 earthquake are estimated at 17 billion dollars, with estimated deaths of 3,000 to 14,000, depending upon the time of day of the earthquake (FEMA, 1980). Because the 1857 earthquake occurred on the San Andreas fault, the nearest point of which is about 50 km northeast of the densely populated area of Los Angeles, a smaller earthquake, in the magnitude range of 7 to $7\frac{1}{2}$, occurring within an urban area may be expected to cause losses comparable to or greater than those for a repeat of the great 1857 earthquake. For example, a future large earthquake in a metropolitan area of California is expected to result in up to 60 billion dollars in property loss and 3,000 to 23,000 deaths [*Danforth*, 1987].

The probabilities computed for this report are based upon a model for time–dependent increase of earthquake probability. The model has its origin in the cycle of stress accumulation and release that characterizes the earthquake cycle. Following an earthquake large enough to rupture an entire segment of a fault (termed a characteristic earthquake) we assume the potential for a future large earthquake along that fault segment is initially small and that it increases as a function of time as the motion of the earth's crust again builds the stress on the fault toward the limit for failure. These properties of recurring earthquakes are qualitatively expressed in the seismic gap hypothesis, which states that the potential for a future earthquake is greater along those active fault segments having large elapsed times since the last characteristic earthquake. Since 1968, 13 large and great earthquakes have occurred in the Circum-Pacific region at sites previously identified by the application of the seismic gap hypothesis [*Nishenko*, 1989].

In the past decade, quantitative methods for calculating this increasing, time-dependent probability for earthquake recurrence have received increasing emphasis within the National Earthquake Hazards Reduction Program. Concurrent with research to develop these methods, new results have added to the usable data for application to specific fault segments in California. The further development of analytical techniques and the compilation of seismological and geological data have enabled us to revise and update the earlier time-dependent estimates for selected California faults computed by *Lindh* [1983] and *Sykes and Nishenko* [1984].

The scope of this study was limited to determining the time-dependent probability for large earthquakes originating on the major faults of the San Andreas fault system. In addition to the principal trace of the San Andreas fault, we considered earthquakes originating on the Hayward fault of northern California, and the San Jacinto and Imperial faults of southern California.

There are numerous other active faults in California, some certainly capable of producing large earthquakes. Figure 1 shows Quaternary active faults in California; the faults drawn in bold lines are those considered for this report. The Working Group concluded that, at this time, there are insufficient data for application of the methods of time-dependent probability calculation to the other faults. Forecasting earthquake occurrence for the other recognized faults in California at present can only be approached by seismic hazard models that do not take into account the length of time since the previous earthquake, and that assume the hazard for an earthquake on any fault remains constant with time (for example, *Algermissen and others*, 1982; and *Wesnousky*, 1986). Individually, these other faults present a lesser potential than do the major faults of the San Andreas system, because the long-term slip rates, historical rates of earthquake occurrence, and earthquake size are much less than those for the faults selected for evaluation. Collectively, however, these faults may present a hazard comparable to those studied in this report.

The recent moderate earthquakes in Whittier and Coalinga, California, serve as a reminder that not all active faults have been recognized everywhere in California. Although almost all well-studied California earthquakes of magnitude 7 and larger have, in fact, occurred on faults having clear surface expression, some faults capable of events of this size have not been identified. This is particularly true in the Transverse Ranges of southern California, where shallowly dipping thrust faults and major folds dominate the tectonic environment, and where the configuration of faults at depth is known to be exceedingly complicated. Thus, we emphasize that not all potential sources of large California earthquakes have been identified in our probabilistic analyses. In view of the limitations that prevented consideration of all potential large earthquakes, the reader should be aware that the total probability for large earthquakes affecting a specific region may significantly exceed the probabilities we present.

In assessing the various fault segments, the Working Group was concerned principally with large earthquakes capable of producing major damage. Several considerations led us to examine earthquakes somewhat below the magnitude 7 cutoff, which is the usual lower limit for earthquakes characterized as large. The principal reason for considering earthquakes having expected magnitudes somewhat less than 7 is that the societal impact of a magnitude 6.8 earthquake originating in a densely populated area, such as the urban corridor along the east side of San Francisco Bay, could be as great or greater than the impact of a magnitude 8 earthquake in a less densely populated area.

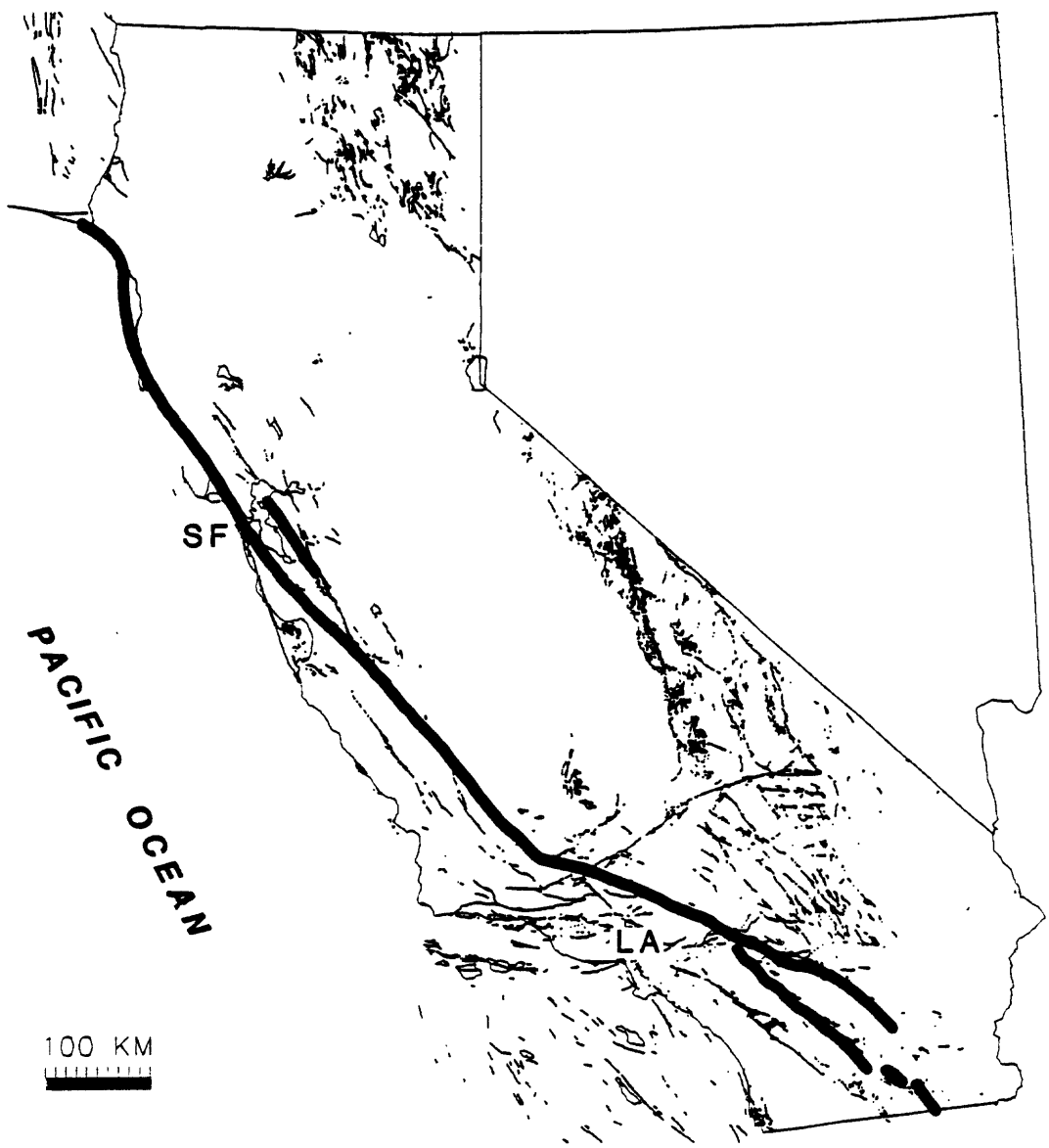

Figure 1. Quaternary active faults in California.

page 9 follows

METHOD AND INPUT PARAMETERS

In the probabilistic calculations presented here, we assume that the probability of the recurrence of an earthquake on a fault segment increases with time. Earthquakes are understood to occur when continuing tectonic motion causes the stresses acting on the fault segment to increase to the point required for rupturing. Uncertainty in our knowledge of the time at which the stress will reach the critical state for the next earthquake necessitates a probabilistic approach. Large earthquakes dominate the pattern of stress release along faults. Consequently, immediately following such an event, the potential for the next large earthquake on the same fault segment is initially small. The probability increases as stress increases and again approaches the failure limit for the next event. Therefore, both the amount of time elapsed since the last large earthquake occurring on a fault segment and the estimated recurrence interval for the next large earthquake on that fault segment affect assessments of earthquake hazard. These time-dependent characteristics distinguish the probability models employed in this study from time-independent hazard models that use only information about recurrence intervals to formulate probability estimates and assume that conditional probabilities are constant with time.

METHOD

The calculation of time-dependent earthquake probabilities requires a probability density function for the expected recurrence interval, $f(T)$. The probability density function and its associated measure of variability, the standard deviation, σ, define the degree of temporal resolution of the expected recurrence time. The probability that an earthquake will occur at some time, t, in the interval $(T, T+\Delta T)$ is obtained by integrating the probability density function over that time interval:

$$P(T \leq t \leq T + \Delta T) = \int_{T}^{T+\Delta T} f(t)dt \tag{1}$$

T and t are measured from the time of the last earthquake.

Throughout this report, the earthquake probabilities we present are conditional probabilities that are based on knowledge that some time, u, has already elapsed in the earthquake cycle without the earthquake having already taken place. The conditional probability of an earthquake, provided the earthquake has not occurred before some time, T, is given by the probability of occurrence in the interval $(T, T + \Delta T)$ divided by the probability of the occurrence for all times greater than T:

$$P(T \leq t \leq T + \Delta T | t > T) = \frac{P(T \leq t \leq T + \Delta T)}{P(t > T)} \tag{2}$$

Figure 2 illustrates a probability density function and the relationship between $P(T \leq t \leq T + \Delta T)$ and $P(t > T)$. For all cases reported below, T corresponds to January 1, 1988.

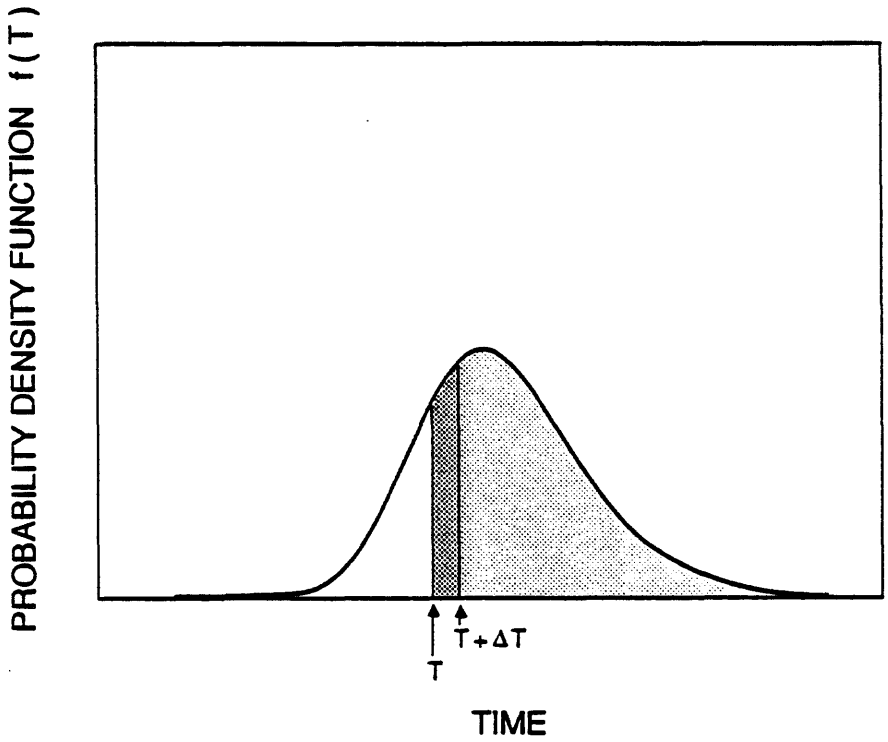

Figure 2. Probability density function for earthquake recurrence. The probability of an earthquake in the interval $(T, T + \Delta T)$ is given by the area of dark shading under the probability density curve. The probability, conditional on the earthquake not having occurred prior to T, is the ratio of the area of dark shading to the sum of the areas with dark and light shading.

Previous studies of time-dependent earthquake hazard have used Gaussian, Weibull, and lognormal probability density functions of recurrence time for computation of conditional probabilities [*Hagiwara*, 1974; *Lindh*, 1983; *Sykes and Nishenko*, 1984; *Nishenko*, 1985; *Nishenko and Buland*, 1987]. In this study, we have employed the lognormal distribution based upon the results of *Nishenko and Buland* [1987], who conclude that the lognormal distribution best represents observed recurrence-time behavior. To evaluate the sensitivity of the results on choice of the probability density function, values were also calculated using the Gaussian probability density. Except for times at the extremes of the distribution functions, well-removed from the mean recurrence time, the differences in probability were not considered significant. For the fault segments studied here, the probabilities calculated using the lognormal distribution generally differ by only a few percent from those obtained using the Gaussian distribution.

The lognormal probability density function employed for this study is:

$$f(T) = \frac{1}{T\sigma\sqrt{2\pi}} e^{-[\ln(T)-(\ln \overline{T}+\mu)]^2/2\sigma^2} \tag{3}$$

where σ is the standard deviation of $\ln(T/\overline{T})$ and $\overline{T}$ is related to the observed average recurrence time, T_{ave}, as $\ln \overline{T} = \ln(T_{ave}) + \mu$. Based upon global analysis of earthquake recurrence, *Nishenko and Buland* [1987] obtain $\mu = -0.0099$. $\overline{T}$ is the recurrence time obtained from the direct method of calculation (the time-predictable model of *Shimizaki and Nakata,* 1980), which uses coseismic slip of the most recent earthquake and long-term slip rate. The method of direct calculation is described more fully below. In *Nishenko and Buland* [1987], the conditional probability is computed from a generic distribution for repeat-time data, conditional on knowing $\overline{T}$, as well as conditional on the event having not yet occurred. However, $\overline{T}$ is itself uncertain because of the limitations in the data used to define $\overline{T}$. For this study, therefore, the probability density function of (3) is constructed as a marginal distribution that implicitly incorporates the uncertainties in $\overline{T}$ into the probability determination. The standard deviation, σ is:

$$\sigma = \sqrt{\sigma_m^2 + \sigma_D^2} \tag{4}$$

where $\sigma_D = 0.21$ is the intrinsic standard deviation of the logarithm of earthquake recurrence times, as determined by *Nishenko and Buland* (1987), and σ_m is the standard deviation of $\ln \overline{T}$, which varies from segment to segment depending upon the nature and quality of input data. Hence, uncertainty in the input data are at least partially accounted for in the probabilities calculated for this report. The marginal probability density, equation (3), becomes more broadly distributed (larger σ) with increasing uncertainty in the data. This broadening of the density function has the effects of damping the changes in conditional probability with time and of reducing the sensitivity of the probabilities to assumptions regarding the input parameters.

The expected recurrence time, T_{exp}, from the distribution function is:

$$T_{exp} = \overline{T} e^{\mu+\sigma^2/2} \tag{5}$$

It is noted that except where σ_m is exceptionally large, $T_{ave} \approx \overline{T} \approx T_{exp}$, with the difference between these parameters generally only 1 to 2 percent.

INPUT PARAMETERS

Application of this method requires the delineation of fault segments expected to slip in large earthquakes; the time of the most recent earthquake from rupture along a fault segment, T_o; the expected recurrence time, T_{exp}, for the next event; and the standard deviation for the probability distribution. A substantial body of seismological

and geological data shows that fault segmentation occurs on a variety of scales and that the style and amount of deformation often repeat on the same part of the fault during successive earthquakes. The behavior of a segment may be characterized by a) elapsed time since the most recent earthquake to rupture the segment; b) recurrence interval; c) amount of slip per event; and d) long-term slip rate. The date of the most recent earthquake and the expected time of occurrence of the next event are based on the types of information that are summarized below and shown in Table 1. The average recurrence time, T_{ave}, is the average of the dates of repeated historical earthquakes known to have ruptured the same fault segment or from geologic dating of slip events inferred to represent earthquakes on the same fault segment. From fault displacement information and slip rate, $\overline{T}$ may be directly calculated. Expected magnitudes shown in Table 1 have been rounded to the nearest half magnitude unit. In Table 1, and elsewhere in this report (unless otherwise noted), magnitudes used are based on seismic moment (moment magnitude, see *Hanks and Kanamori* [1979]).

The earthquake and fault displacement data used to obtain the probabilities come from a variety of sources, each with its own set of uncertainties that affect the reliability of the probability determinations. The Appendix to this report reviews the different types and sources of earthquake and fault displacement data and discusses their applicability to earthquake forecasting.

Conditional probabilities are sensitive to the segmentation models used. For most of the fault segments discussed below, data employed to define a segment are sparse and data obtained at one point on a fault are sometimes extrapolated 100 km or more. For these reasons, there is often significant uncertainty in the identification of fault segments. For example, a single fault segment that we have identified may in fact consist of two segments that will generate two smaller separate earthquakes. Similarly, two or more adjacent segments may slip in a single large earthquake. The segments described in this report represent our best judgment using present data to define these source regions for probabilistic assessments.

For some of the expected earthquakes, the concept of a characteristic earthquake [*Schwartz and Coppersmith*, 1984; *Bakun and McEvilly*, 1984; *Wesnousky and others*, 1983] could be employed to specify the location of faulting, earthquake magnitude, T_{ave}, and the time of the last earthquake, T_o. A fault segment is said to have a characteristic earthquake if it repeatedly slips in earthquakes of similar magnitude and if those earthquakes dominate the stress release for that segment.

In other cases, the evidence for a characteristic earthquake was either severely limited or the evidence indicated that the next earthquake was expected to differ significantly from the previous event. In those cases, segment delineation was based additionally upon a combination of observations and judgments that are described below in the discussion of specific fault segments, and recurrence time was directly estimated from fault displacement and long-term slip rate.

The date of the most recent earthquake, T_o, is known from either historical or geological data for most of the fault segments considered in this study. For fault segments

Table 1

Raw Data for Recurrence Time Calculations

Fault Segment	Date of Most Recent Event	Length (km)	Slip Rate (mm/yr $\pm 1\sigma$)	Displacement (cm$\pm 1\sigma$)	Coefficient Variation(σ)	Expected Magnitude	Method
San Andreas Fault							
North Coast	1906	360	16 ± 2.5	450 ± 100	0.41	8	Direct
San Francisco Peninsula	1906	90	16 ± 2.5	250 ± 60	0.42	7	Direct
S. Santa Cruz Mtns.[1]	1906	35	16 ± 2.5	200 ± 50	0.43	6½	Direct
Parkfield	1966	30			0.24	6	Historical
Cholame	1857	55	34 ± 1.5	475 ± 200	0.53	7	Direct
Carrizo	1857	145	34 ± 1.5	950 ± 200	0.37	8	Direct
Mojave	1857	100	30 ± 5	450 ± 100	0.41	7½	Direct
San Bernardino Mtns.	1812(?)	100	24 ± 3	400 ± 100	0.60	7½	Direct
Coachella Valley	1680 ± 20	100			0.30	7½	Geologic
Hayward Fault							
Northern East Bay	1836(?)	50	7.5 ± 2.0	140 ± 40	0.50	7	Direct
Southern East Bay	1868	50	7.5 ± 2.0	140 ± 40	0.50	7	Direct
San Jacinto Fault							
San Bernardino Valley	1890(?)	50	8 ± 3	140 ± 40	0.56	7	Direct
San Jacinto Valley	1918	65	11 ± 3	180 ± 50	0.50	7	Direct
Anza	1892(?)	50	11 ± 3	140 ± 40	0.50	7	Direct
Borrego Mountain	1968	50	4 ± 1	70 ± 20	0.42	6½	Direct
Imperial Fault							
Imperial	1979	30	30 ± 5	120 ± 40	0.48	6½	Direct

[1] Southern subsegment of San Francisco Peninsula segment.

where the date of the last event is not known, we have assigned dates based on either our interpretation of the historical record (as in assigning the 1836 earthquake to a specific segment of the Hayward fault), or dates that represent the beginning of systematic reporting in a particular area. In the latter case, probability values based on these dates represent minimum values, as the event in question may have occurred considerably earlier. This latter situation applies commonly to segments of the San Jacinto fault, where the period of consistent reporting of moderate events starts in the 1890's.

The average or expected recurrence times are estimated from either the historical/ geological record or from direct calculations. Although historical accounts provide the principal data base for studies of this kind, their application is limited. The short duration of the written record for various parts of California (90 to 200 years) severely limits the widespread use of historical data for estimating recurrence times. In fact, only one of the 18 segments considered in this study has a history of three or more earthquakes (two or more recurrence intervals). This is the Parkfield fault segment.

Our understanding of fault activity and fault behavior has increased by the application of seismic geology and paleoseismicity investigations along various fault segments, using trenching and geomorphic techniques to gather data for analysis and interpretation. The results of these studies have greatly extended the record of earthquake activity in southern California. Errors in ^{14}C dating and the identification and correlation of these prehistoric events from site to site, however, introduce uncertainty into T_{ave}. Both historical and geological data for two or more large earthquakes can be used to constrain recurrence times and hazard estimates for 3 of the 17 segments discussed in this report. These are the Parkfield, Mojave, and Coachella Valley segments.

For those fault segments where historical and geological data are insufficient to compute T_{ave}, we have estimated recurrence times based on the size of the most recent earthquake along a given fault segment. These direct estimates of recurrence time, $\overline{T}$, assume the time-predictable earthquake hypothesis [*Shimizaki and Nakata,* 1980] and are obtained by dividing the slip during the most recent earthquake by the long-term fault slip rate. Examples of these types of calculations can be found in *Sykes and Quittmeyer* [1981], *Sykes and Nishenko* [1984] and *Nishenko* [1985]. Uncertainties in our estimates of the coseismic displacement and long-term rates of displacement increase σ, resulting in broader probability densities that in turn limit the temporal resolution from these types of data.

For the Hayward fault segments and several of the San Jacinto fault segments, observations of slip distribution are sparse or nonexistent. For those segments, the fault displacements used for the direct calculation of $\overline{T}$ were constrained to be compatible with length/displacement scaling relationships and data for strike-slip earthquakes [for example, *Dieterich*, 1974; *Kanamori and Anderson*, 1975; *Scholz*, 1982; *Bonilla and others*, 1984]. The Hayward and San Jacinto fault segments in question all have lengths, L, of 50 to 65 km. We have employed displacements for those segments as given by the relation: $D = 2.8 \times 10^{-5} L$. This relationship yields displacements that are about 80 percent of those obtained from the *Bonilla and others* [1984] relationship for maximum displacement

in strike-slip earthquakes, and yields displacements that are roughly twice those given by the relationship of *Scholz* [1982] for average displacement in strike-slip earthquakes. However, for fault lengths of 50 to 100 km, the average displacement data of *Scholz* [1982] are all greater than his reported length/displacement relationship. Our assumed values therefore slightly exceed the upper bound for the average displacements on fault segments of this length. In general, the standard deviation of the density functions associated with these direct estimates are a factor of 1.5 to 2.0 larger than the standard deviations for historically based recurrence time data. Overall, these direct calculations are used for 14 of the 17 segments considered in this study.

page 17 follows

RESULTS OF PROBABILITY CALCULATIONS

Figures 3 and 4 and Table 2 summarize the results of the probability calculations for the fault segments listed in Table 1. Below, each of these fault segments is discussed in detail. The time interval chosen for the probability calculations spans the 30 years from the beginning of 1988 to 2018.

Limitations and gaps in the data introduce unavoidable uncertainty into delineation of fault segments and computed probabilities. The marginal distribution used to compute the probabilities accounts for some, but not all uncertainties in the data. In particular, possible segment mischaracterizations or alternate segmentation models that may lead to significantly different expected magnitudes and recurrence times are not explicitly represented in σ as given in Table 1. To distinguish fault segmentation models based upon relatively good data from those based on poor or incomplete data, each segment has been given a letter grade from A to E in Table 2. The segments judged to have the most reliable data are ranked A; E indicates the least reliable data. For a level of reliability of E, the earthquake probability obtained from application of the time-dependent model is judged to be only slightly more reliable than the probability obtained from application of time-independent probability models. For levels of reliability of C, D, and E, both the evaluation of segment length (and the related expected magnitude) and the probability value may change significantly with additional data. For most fault segments, values of σ (Table 1) and the letter grades correlate. Hence, low values of σ are associated with high level of reliability letter grades (A, B) and high values of σ are associated with poor letter grades (D, E). In a few cases, this rule does not hold, as with the Southern Santa Cruz Mountains segment of the San Andreas fault, where the data for most recent earthquake (displacement and slip rate) are relatively good, resulting in a low σ, but where the validity of the segmentation model is judged highly uncertain, resulting in a poor letter grade (E).

Within a region containing more than one fault segment, the total probability of the occurrence of at least one large earthquake is, for many applications, of greater interest than the probabilities for the individual segments. Table 3 presents the results of aggregating the individual probabilities to forecast the probability of at least one earthquake for several regions. The regions chosen are the San Francisco Bay Area, the southern San Andreas fault, and the San Jacinto fault. The probability for one or more earthquakes originating within an area, obtained by aggregating the probabilities for earthquakes on the individual segments, is referred to as the total probability in the following discussion. The total probabilities of one or more events within 5-, 10-, 20-, and 30-year intervals are obtained from:

$$P = 1 - (1 - P_a)(1 - P_b)(1 - P_c)\cdots \tag{6}$$

where P_a, P_b, and P_c are the individual conditional probabilities for earthquakes on segments a, b, and c, respectively, for the time interval of interest. Note that $(1 - P_a)$, $(1 - P_b)$, and $(1 - P_c)$ are the probabilities for segments a, b, and c not experiencing earthquakes during the time interval in question. The probability, P, as given by equation

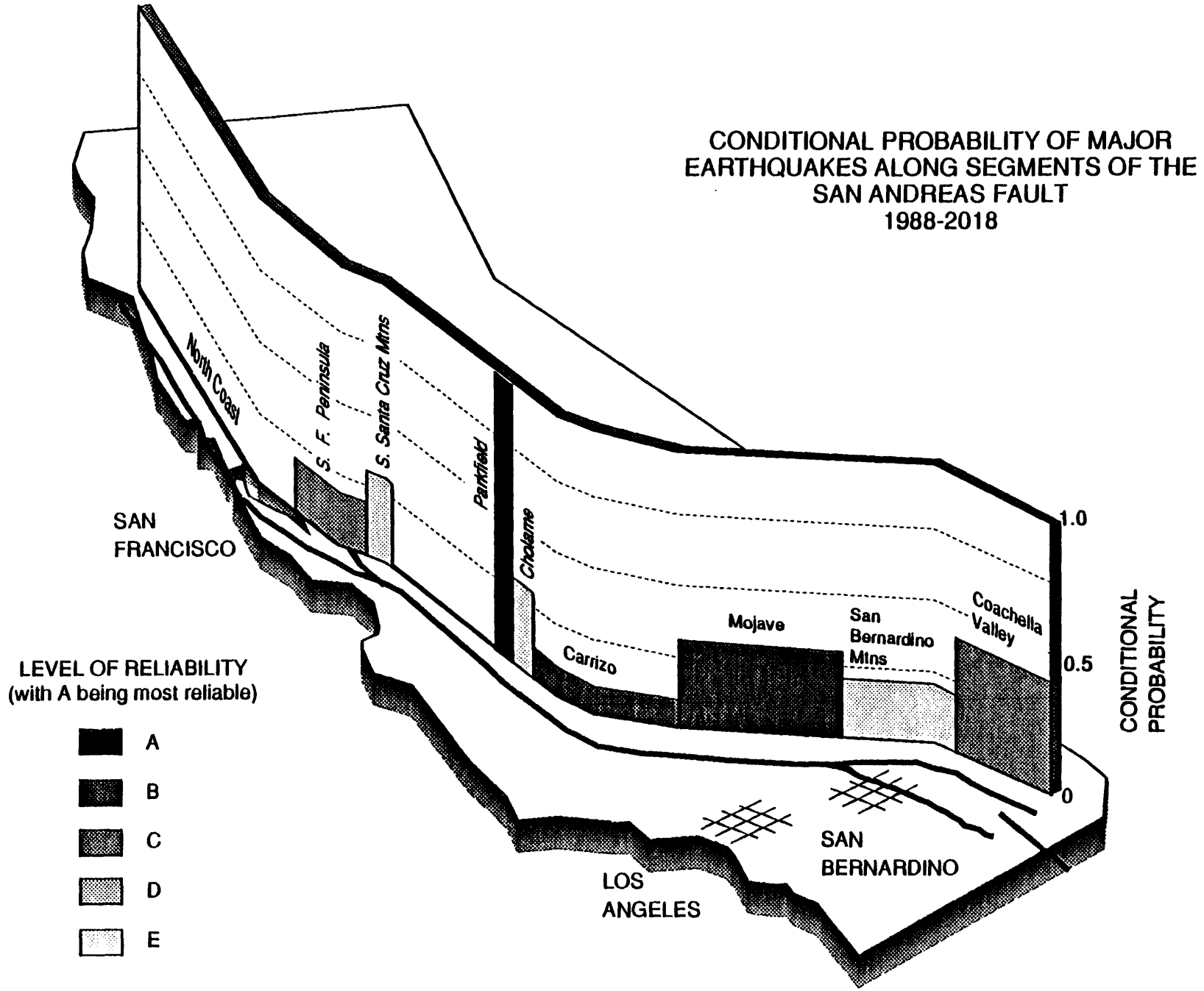

Figure 3. Conditional probability for the occurence of major earthquakes along the San Andreas fault, in the 30-year interval from 1988 to 2018. See text for description of the fault segments.

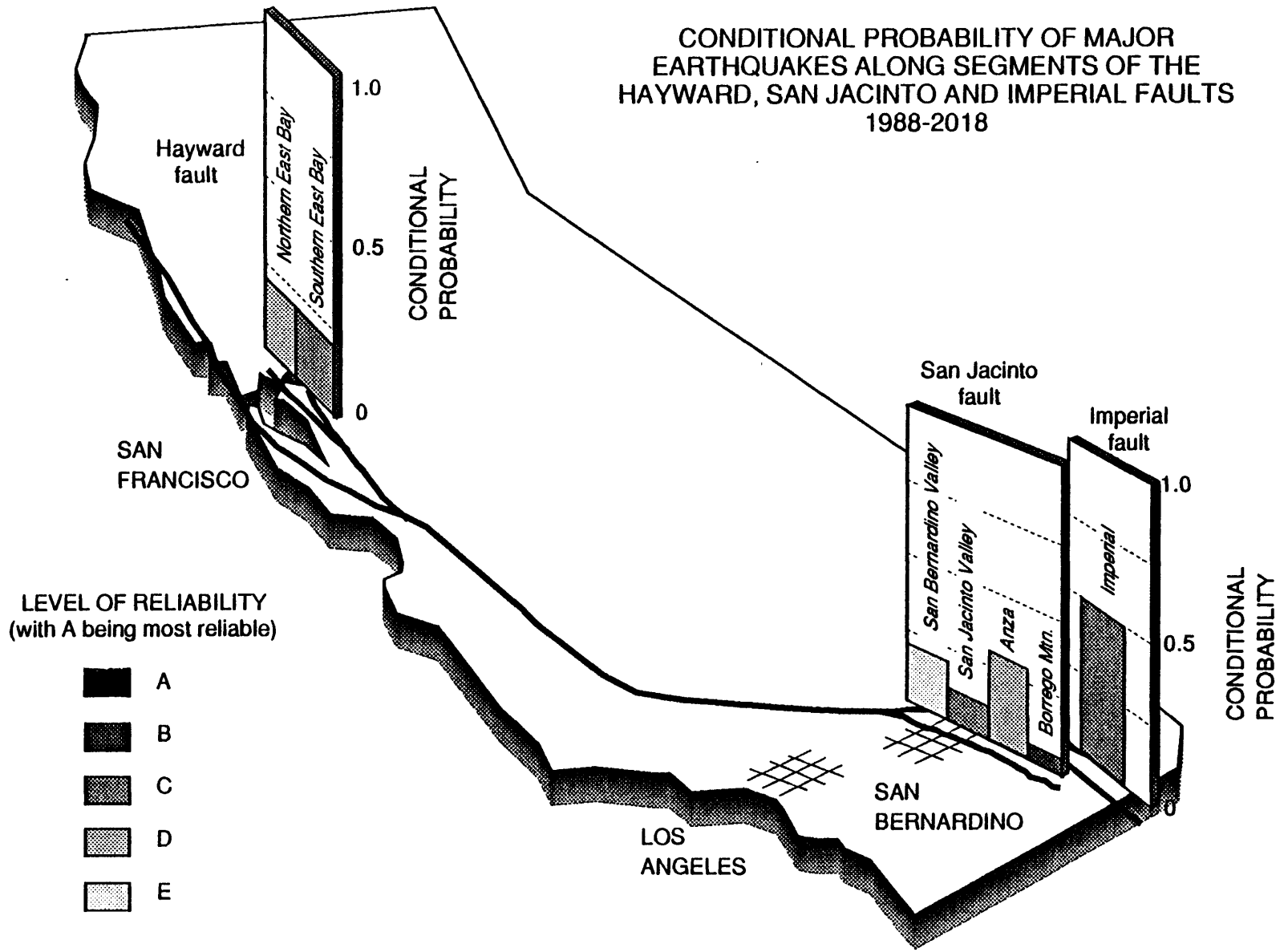

Figure 4. Conditional probability for the occurence of major earthquakes along the Hayward, San Jacinto, and Imperial faults, in the 30-year interval from 1988 to 2018. See text for description of the fault segments.

Table 2

Recurrence Times and Conditional Probabilities of Earthquakes

Fault Segment	Date of Most Recent Event	Expected Magnitude	Expected Recurrence Time (yrs)	Conditional Probability 1988–2018	Level of Reliability (A most reliable)
San Andreas Fault					
North Coast	1906	8	303	<0.1	B
San Francisco Peninsula	1906	7	169	0.2	C
S. Santa Cruz Mtns.	1906	6 1/2	136	0.3	E
Central Creeping				<0.1	A
Parkfield	1966	6	21	>0.9	A
Cholame	1857	7	159	0.3	E
Carrizo	1857	8	296	0.1	B
Mojave	1857	7 1/2	162	0.3	B
San Bernardino Mtns.	1812(?)	7 1/2	198	0.2	E
Coachella Valley	1680±20	7 1/2	256	0.4	C
Hayward Fault					
Northern East Bay	1836(?)	7	209	0.2	D
Southern East Bay	1868	7	209	0.2	C
San Jacinto Fault					
San Bernardino Valley	1890(?)	7	203	0.2	E
San Jacinto Valley	1918	7	184	0.1	C
Anza	1892(?)	7	142	0.3	D
Borrego Mountain	1968	6 1/2	189	<0.1	B
Imperial Fault					
Imperial	1979	6 1/2	44	0.5	C

Table 3

Probability of One or More Large Earthquakes on Faults of the San Andreas Fault System

Geographic Region or Fault	Expected Magnitude	Probability For Intervals Beginning 1/1/88			
		5 yr	10 yr	20 yr	30 yr
San Francisco Bay Area					
Including the San Francisco Peninsula segment of the San Andreas fault and the Northern East Bay and Southern East Bay segments of the Hayward fault	7	0.1	0.2	0.3	0.5
Southern San Andreas Fault[1]					
Mojave and Coachella Valley segments	7 1/2–8	0.1	0.2	0.4	0.6
San Jacinto Fault					
San Bernardino Valley, San Jacinto Valley, and Anza segments	6 1/2–7	0.1	0.2	0.3	0.5

[1] The total probabilities listed here for the southern San Andreas fault assume the San Bernardino Mountains segment does not have earthquakes independent of the Mojave or Coachella Valley segments. If earthquakes along the San Bernardino Mountains segment are independent of other segments, then the total probabilities for the southern San Andreas fault increase to 0.2, 0.3, 0.5, and 0.7 for 5, 10, 20, and 30 years, respectively.

(6) is the total probability that segment a and/or segment b and/or segment c will have an earthquake in the time interval. Application of equation (6) to combine the probabilities within a region assumes independence of the individual probabilities. After computing the values in Table 3, they were rounded to a single significant figure.

The application of (6) to aggregate probabilities of segments having different data quality grades may give unwarranted weight to segments having poor data quality if the individual probabilities for those segments do not fully take in account the uncertainties in the data. We have attempted to account for data uncertainties in the calculation of the probabilities; however, the possibility exists that some segmentation models are incorrect. The total probability obtained by application of (6) will be an upper limit if the aggregation includes segments whose earthquakes could be dependent upon earthquakes in other segments. In this regard, the inclusion of E-quality segments, particularly San Bernardino Mountains and Cholame segments where the characteristic earthquake is most uncertain and which may not have independent earthquakes (see discussion below), may tend to bias the aggregated total probabilities upward. However, eliminating the San Bernardino Mountains and Cholame segments from the aggregated total probabilities does not have a large effect on total probability. In Table 3, we report the total probabilities for one or more large earthquakes ($M = 7\,1/2$ to 8) on the southern San Andreas fault without the San Bernardino Mountains segment. Including the San Bernardino Mountains segment into the aggregation for the southern San Andreas fault increases the 5-, 10-, 20-, and 30-year probabilities from 0.1, 0.2, 0.4, and 0.6, respectively, to the upper limit of 0.2, 0.3, 0.5, and 0.7, respectively. We note that the behavior of the San Bernardino Mountains segment could critically affect the size of the expected earthquakes. If earthquakes along the Mojave or Coachella Valley segments cause the San Bernardino Mountains segment to slip at the same time, or vice versa, then significantly larger earthquakes approaching the size of the great earthquake of 1857 will result.

For comparative purposes, we have also computed total probabilities from the time-independent Poisson model, using the recurrence times obtained from the data of Table 1 and time-dependent total probabilities for previous intervals beginning in 1920. For the segments listed as San Francisco Bay Area in Table 3, the 30-year Poisson total probability is 0.4. The 30-year probability for one or more earthquakes from the time-dependent method was 0.2 in 1920, increasing to 0.5 at the beginning of 1988. For the southern San Andreas (San Bernardino Mountains segment excluded) the total 30-year Poisson probability is 0.3 and the time-dependent probability varied from 0.4 in 1920 to 0.6 in 1988. Along the San Jacinto fault, the total 30-year probability from the Poisson model is 0.4 and the 30-year time-dependent total probability varied from 0.1 in 1920 to 0.5 in 1988. We note that each of these areas has been seismically quiet for most of this century, that the total time-dependent probabilities in 1920 were low, and that, at present, the total probabilities have increased to levels above the Poisson probabilities.

FAULTS OF THE NORTHERN SAN ANDREAS FAULT SYSTEM

We focus here on the major strike-slip faults of the San Francisco Bay Area and also consider their northerly and southerly extensions toward Olema and Hollister, respectively (Figure 5). Choice of segments depends largely on evidence from historical large earthquakes: the coseismic slip distribution for the great San Francisco earthquake and subjective judgment for the location and slippage in the 1836 and 1868 events of about magnitude 7 on the Hayward fault. These segments are shown in Figure 5 and are listed below:

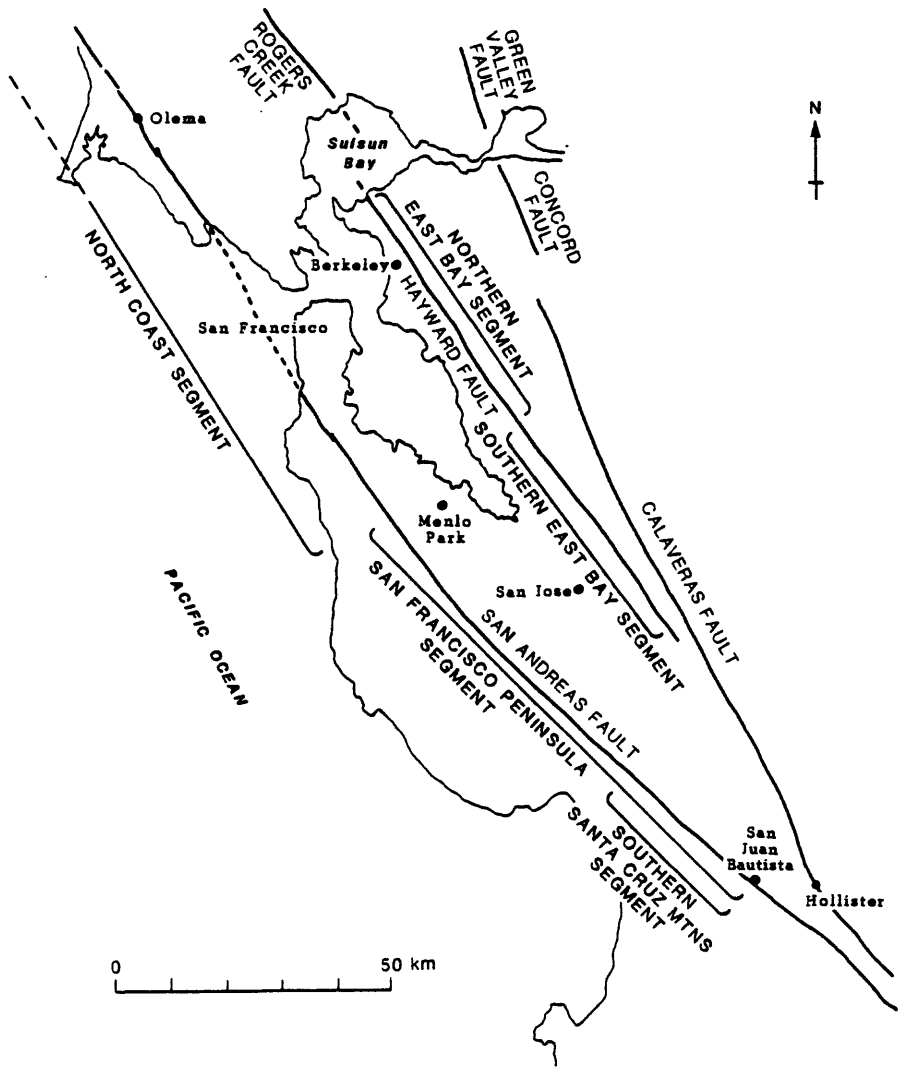

Figure 5. Segments of the major strike-slip faults of the northern San Andreas fault system.

Segment (Fault)	Length (km)	Basis of Distinction
1. North Coast (San Andreas)	360	4 to 7 m slip in 1906
2. San Francisco Peninsula (San Andreas)	90	<3 m slip in 1906
3. Southern Santa Cruz Mountains (San Andreas)	35	End zone of 1906 rupture
4. Northern East Bay (Hayward)	50	Presumed site of 1836 earthquake
5. Southern East Bay (Hayward)	50	Presumed site of 1868 earthquake

Northern San Andreas Fault

Probability calculations for the northern San Andreas fault depend critically on the slip distribution during the most recent faulting event, the great 1906 earthquake, and the amount of strain accumulated since then. Geodetic and surface measurements of slip in the 1906 earthquake are 4 to 7 m over most of the 450-km-long extent of slippage (Figure 6). Figure 6 shows the geodetically measured slip as straight-line segments with one standard deviation error bars (plot modified from *Thatcher and Lisowski*, 1987*b*). The southernmost 125 km of the 1906 rupture has received special attention in studies of long-term seismic potential, because in this region, 1906 slip decreased from about 5 m near San Francisco, to near zero at San Juan Bautista. A significant portion of this 125-km-long section of the San Andreas also slipped in 1838 causing an earthquake of about magnitude 7, although the amount of slippage and the extent of rupture are not known [*Louderback*, 1947].

North Coast Segment. The 360-km-long reach of the 1906 rupture, where slip was more than about 4 m, has been considered as a single segment. Long-term slip rate, 16 ± 2.5 mm/yr, is the same as that derived for the San Francisco Peninsula segment (see discussion below). Given this slip rate and a coseismic slip of 4.5 ± 1.0 m, the probability of a large earthquake on the entire segment in the next 30 years is very low, less than 0.1. However, the earthquake of 1898 off Pt. Arena ($M = 6.7$) and possibly the earthquake of 1915 located farther offshore ($M = 6.2$) indicate that this segment, especially north of Point Arena, should be considered capable of generating smaller earthquakes at any time.

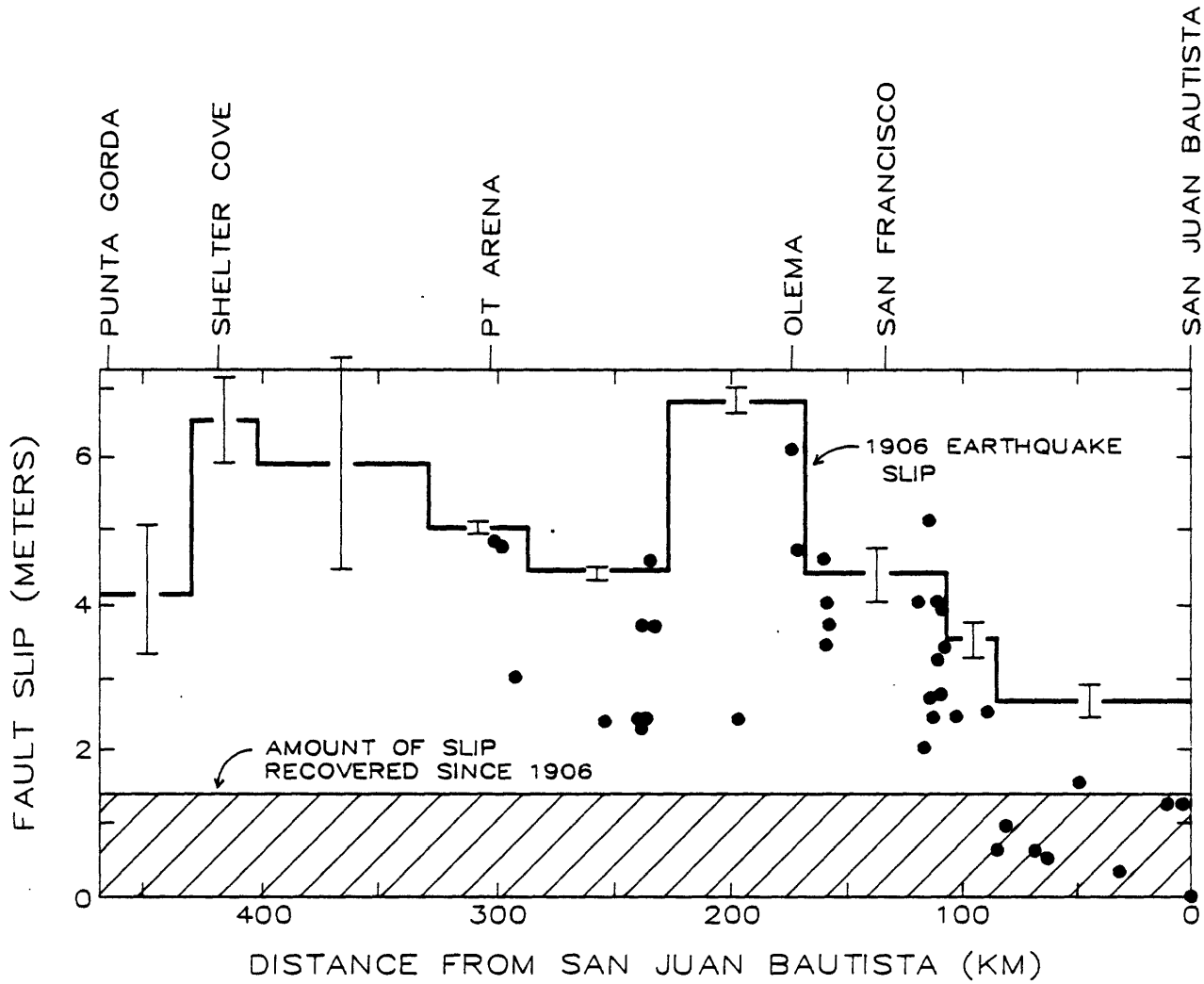

Figure 6. Slip measured on the San Andreas fault following the great 1906 San Francisco earthquake. Solid dots show surface fault offsets; straight line segments indicate geodetic measurements of fault slip, with one–standard–deviation error bars shown for each determination. Rectangle with diagonal hatching at bottom of graph indictes amount of slip recovered by elastic strain accumulation since 1906 (that is, the long-term slip rate of 16 mm/yr multiplied by the 82 years that have elapsed since 1906).

San Francisco Peninsula Segment. Measured offsets of fences and other cultural features are available for about 310 km of the 1906 fault rupture (solid dots, Figure 6), and except for the southernmost 90 km of rupture, their maximum values agree well with geodetically derived slip estimates (straight-line segments with one standard deviation error bars, Figure 6). The departure of the two slip estimates on the southern San

Francisco Peninsula segment is important from the standpoint of long-term probability because they differ by a factor of two (geodetic: 2.6 ± 0.3 m, fault offsets: 1.5 m or less). Figure 6 illustrates how the fault offset data used by *Sykes and Nishenko* [1984] and by *Scholz* [1985] suggest that the hazard on the southernmost 90 km of the 1906 rupture may be high. If a long-term slip rate of 16 mm/yr is assumed (see below), elastic strain accumulated since 1906 now almost equals the observed 1.5 m surface fault offset of 1906. Thus, if the fault offset values are appropriate, an event of about magnitude 7 may have a high probability during the next few decades [*Sykes and Nishenko*, 1984; *Scholz*, 1985]. Conversely, if the larger, geodetically determined coseismic slip is more nearly correct, such an event is not expected until the mid or late 21st century [*Lindh*, 1983; *Thatcher and Lisowski*, 1987*a*].

The origin of this slip discrepancy has been examined recently by *Thatcher and Lisowski* [1987a], who argued that the geodetic slip estimates are more reliable than the fault offset values on this 90-km-long segment. They found that the geodetic slip could not be significantly reduced by modifying fault modeling assumptions. They also showed that the survey measurements themselves were precise enough to define slip within a narrow range. At the same time, *Thatcher and Lisowski* concluded that the fault offset values were biased on the low side because of the considerable width and complexity of this reach of the San Andreas fault zone, which differs in trend by about 6 degrees from the much narrower and simpler fault zone extending 220 km to the northwest.

The Working Group felt that although there was room for doubt, the geodetically determined coseismic slip value was the more appropriate to apply to probabilistic hazard calculations for this segment. However, the several model calculations carried out by Thatcher and Lisowski suggest larger uncertainties than are indicated by their preferred estimate of 2.6 ± 0.3 m, and a value of 2.5 ± 0.6 m was adopted for our probability calculations. As well as doubling the formal error bounds, this places the adopted value within two standard deviations of the maximum fault offset measurements.

Geologic [*Hall*, 1984; *Cummings*, 1983] and geodetic data [*Prescott and others*, 1981; *Prescott and Yu*, 1986; *Thatcher*, 1979] give slip rates ranging from about 8 to 15 mm/yr on the San Andreas fault in the San Francisco Bay region. However, several of these estimates might be fairly regarded as minimum values. Furthermore, if the full San Andreas slip rate of 33 ± 1 mm/yr, measured across the Central Creeping segment of the fault [*Thatcher*, 1979] is to be accommodated on only the Hayward–Calaveras and San Andreas faults in the San Francisco Bay area, northern San Andreas slip rates could credibly be as great as 20 mm/yr. To include this range of possibilities in a single slip-rate estimate, we have thus adopted a value of 16 ± 2.5 mm/yr.

Using the adopted values of 2.5±0.6 m and 16±2.5 mm/yr for 1906 slip and long-term slip rate we obtain a 30-year conditional probability of 0.2, which is assigned a level of reliability rating of *C* in Table 3. For comparison, if we use the same slip rate and the maximum fault offset of 1.5 m (±0.5 m), we obtain a probability of 0.4. Although this difference is still significant, use of the larger data variances assumed in this report has

notably dampened the range of the calculated probabilities, as previously quoted values varied from .06 to .95 [*Sykes and Nishenko*, 1984; *Thatcher and Lisowski*, 1987*a*].

The 1838 earthquake, of estimated magnitude 7 [*Toppozada and others*, 1981], was centered in the southern San Francisco Peninsula [*Louderback*, 1947], and it may well have been associated with local rupture of the San Andreas fault comparable to that of 1906 on this segment. Inasmuch as these two events were only 68 years apart, one might question the 169-year recurrence time shown in Table 2. On the other hand, one could argue that the 1838 and 1906 earthquakes were mechanically closely coupled, and that a more appropriate recurrence time is that of the North Coast segment, 303 years. We support the intermediate value of 169 years, recognizing its significant uncertainty.

Southern Santa Cruz Mountains Segment. The possibility of a somewhat smaller event, magnitude $6\frac{1}{2}$ to 7, on the southernmost ~30 km of the 1906 rupture is equivocal. Such an event, similar to that proposed by *Lindh* [1983], is suggested both by the proximity to the Central Creeping segment of the San Andreas and by the occurrence of historical earthquakes of about this size in 1865 and 1890. The geodetic data bearing on 1906 slip do not preclude slip values that decrease to the observed fault offset values of ~1.2 m on this segment, but neither do they support it. Nonetheless, slip must decrease southward along this segment, although it is at least 1.2 m only 5 km northwest of San Juan Bautista (see Figure 6). As in the case of the northern end of the 1857 fault rupture (Cholame segment, see below), this gradient in coseismic slip makes it questionable to assign a single slip value to the entire segment. However, for illustrative purposes we have taken a slip value near the middle of the range of possibilities, 2.0 ± 0.5 m. Using this value, the date of the 1906 earthquake, and a slip rate of 16 ± 2.5 mm/yr, we find the 30-year probability to be 0.3. Because little is known to constrain the seismic history and slip characteristics of this segment, the probability value is assigned a level of reliability rating of E.

Hayward Fault

The Hayward fault presents two paradoxes with regard to estimating the time and the place of future damaging earthquakes. Two events of about magnitude 7 occurred on the fault in the past 150 years, in 1836 and 1868, suggesting that over the long term such events might be expected as frequently as one or two per century [*Lawson and others*, 1908; *Louderback*, 1947]. On the other hand, *Prescott and Lisowski* [1982] have argued that although as much as 10 mm/yr of displacement has been measured geodetically across the Hayward fault during the past 15 years, most of this displacement may be explained by aseismic slip (creep), implying to them that little or no elastic strain accumulation is occurring. *Nason* [1971] has shown that these slip rates have remained remarkably constant through most of this century.

The second paradox is that the two historical Hayward earthquakes occurred only 32 years apart, and yet 120 years have passed since the last one. Either this implies an extremely irregular recurrence pattern on a single segment, or the two 19th century events occurred on two different segments of the Hayward fault.

Estimating an average recurrence interval on the Hayward fault is further complicated by the fact that there are no published Holocene slip rates or paleoseismic estimates of the occurrence times of prehistoric large events. In view of the high level of cultural development along most of the Hayward fault, this omission will not be easily remedied. However, when taken in concert with the very clear geologic, geomorphic, and microseismic expression of the Hayward fault, the available data clearly indicate that earthquakes up to about magnitude 7 will occur there in the future. Given that the Hayward fault is capable of earthquakes large enough to present a serious threat to society, and that enough time has passed since the last one, the possibility of a large earthquake should be a serious societal concern.

Northern and Southern East Bay Segments. In an attempt to force onto this fragmentary picture a coherent recurrence pattern, we have made a number of plausible assumptions. First, we have placed the two historical Hayward earthquakes on adjacent 50-km-long segments [*Lindh*, 1983], named here the Northern East Bay (last event in 1836) and Southern East Bay (last event in 1868) segments. Using the empirical fault-length/ displacement relation discussed above, we have assigned coseismic slip values of 1.4 ± 0.4 m to both these segments. We have taken a slip rate of 7.5 ± 2.0 mm/yr as representative of the Hayward fault. This estimate includes within its one-standard-deviation bounds *Prescott and Lisowski's* [1982, 1983] determination of surface creep rate (6 mm/yr), and it is within two σ of their upper bound on the rate of geodetic displacement, 10 mm/yr. Using this rate in recurrence and probability calculations implicitly assumes the existence of two ~50-km-long segments locked at depth on the Hayward fault that have sustained little if any slip since the earthquakes of 1836 and 1868.

We thus calculate the probability of a characteristic event within the next 30 years to be 0.2 for the Northern East Bay and the Southern East Bay segments. Given the several uncertainties associated with the Hayward fault, these values must be considered less precise than those for the best-constrained segments on the San Andreas fault. We nonetheless feel that the long-term likelihood of events of about magnitude 7 on the Hayward fault may be high.

Other Faults of the Northern San Andreas Fault System

Calaveras Fault. The 160-km-long Calaveras fault (including the closely related Concord fault, Figure 5) extends from Suisun Bay on the north to its convergence with the Central Creeping segment of the San Andreas southeast of Hollister. Aseismic slippage dominates the behavior of this fault throughout its length [*Prescott and others*, 1981]. However, earthquakes as large as about magnitude 6 have occurred on the Calaveras fault, most recently at two adjacent localities southeast of San Jose in 1979 and 1984. An earlier event of about this magnitude occurred on the northern Calaveras fault in 1861. No events of larger magnitude have occurred in historical time. For the purposes of this report, there is little basis for making probabilistic assessments of long-term potential for earthquakes of magnitude 7 or greater.

North Bay Faults. Recognized Quaternary faults of the North Bay include the Rogers Creek-Healdsberg, Maacama, Green Valley, Berdell Mountain, Tolay, West Napa, and Cordelia faults. Of these, the Rogers Creek-Healdsberg, Maacama, and Green Valley have recognized Holocene displacement and are designated as Alquist-Priolo Special Studies Zones. Although a variety of studies using reconnaissance-level mapping, interpretation of aerial photographs, and trenching for Alquist-Priolo zoning have revealed geomorphic and stratigraphic evidence of repeated late Pleistocene-Holocene displacement, no published studies have been made of these faults for the express purpose of quantifying fault behavior parameters. Presently, there is no information on slip rates, recurrence intervals, amount of displacement during individual earthquakes, or the elapsed time since the most recent large event. No historical earthquakes larger than magnitude 6 have occurred on these faults. Because of insufficient data, none of these faults has been included in a compilation of California slip rates [*Clark and others*, 1984]. For the purposes of this report, there is little basis for making probabilistic assessments of long-term potential for earthquakes of magnitude 7 or greater.

FAULTS OF THE SOUTHERN SAN ANDREAS FAULT SYSTEM

Central and Southern San Andreas Fault

We have divided the southern half of the San Andreas fault into seven segments that, for the reasons outlined in the table below, we believe may differ in their seismic behavior. These segments are shown in Figure 7 and are listed below:

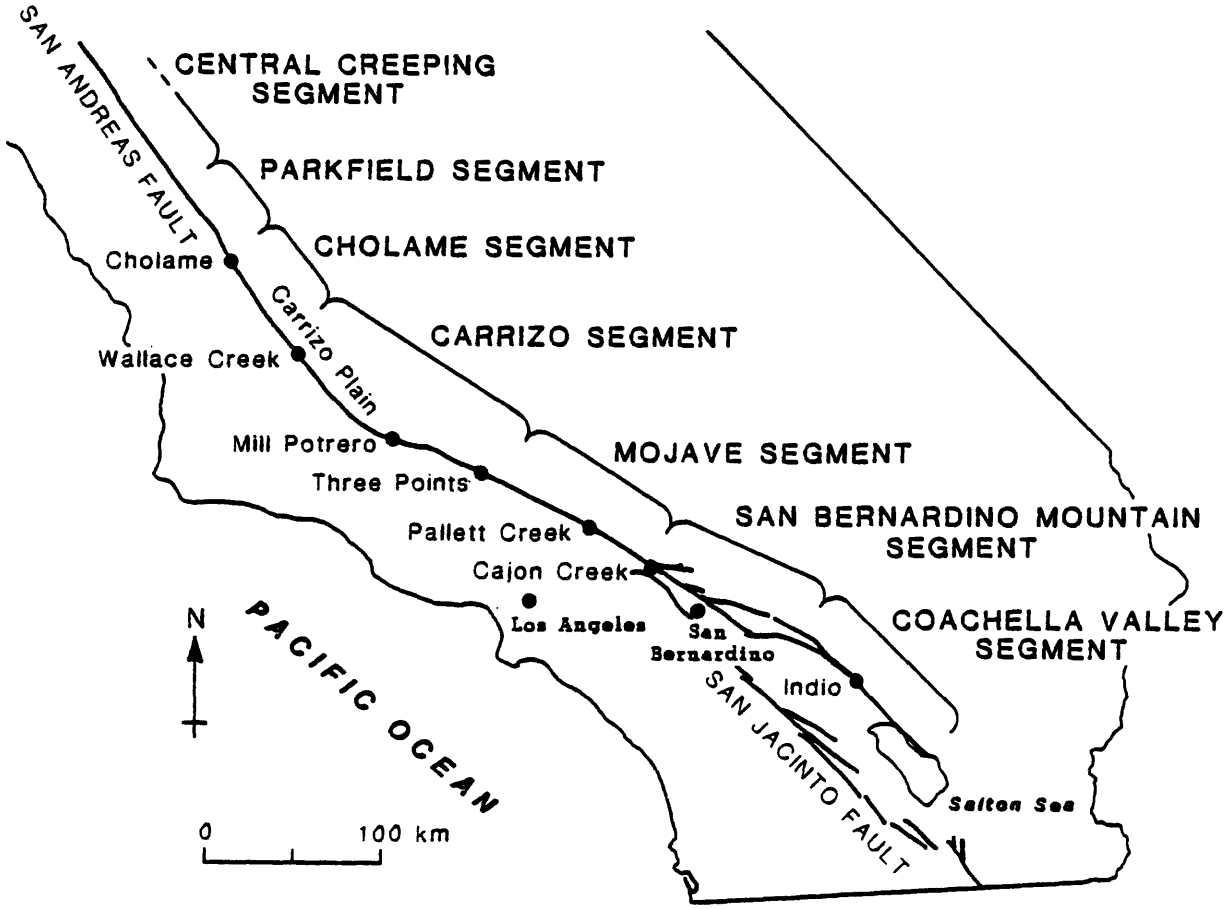

Figure 7. Segments of the central and southern San Andreas fault.

Segment	Length (km)	Basis of Distinction
Central Creeping	130	Historical creep at ~3 cm/yr
Parkfield	30	Transition from Central Creeping segment to locked Cholame segment; M6 quakes about every 22 years
Cholame	55	Transition from high-slip Carrizo segment to low-slip Parkfield segment in 1857
Carrizo	145	High slip (6 to 12 m) in each of past several earthquakes
Mojave	100	Slip of about 4 m in 1857 and probably in previous events
San Bernardino Mountains	100	No certain historical rupture or creep; geometrical complexity
Coachella Valley	100	Historical low-level creep; no certain historical surface rupture; simple geometry

The nature of data bearing upon the earthquake potential of the San Andreas fault in southern California varies greatly among the several segments of the fault. For most segments, so little information is available that calculation of 30-year probabilities must be based upon comparison of potential slip accumulated since the most recent event with estimates of the slip in that event. The earthquake potential of other segments of the fault can be assessed from more abundant historical and paleoseismic data.

An assessment of earthquake potential for the five locked segments of the fault in southern California can be made from the information given in Figure 8. Here, coseismic slip (solid lines) is compared to estimated potential slip (dashed lines). Estimated potential slip is determined by multiplying the estimated long-term slip rate by the years since the latest event. Queries indicate segments for which the data are uncertain. Assuming the likelihood of fault rupture increases as the accumulated potential slip approaches or exceeds the slip of the latest event, Figure 8 should give a rough indication of which segments currently have the highest earthquake potential. The figure clearly points to the high seismic potential of much of the southern San Andreas fault.

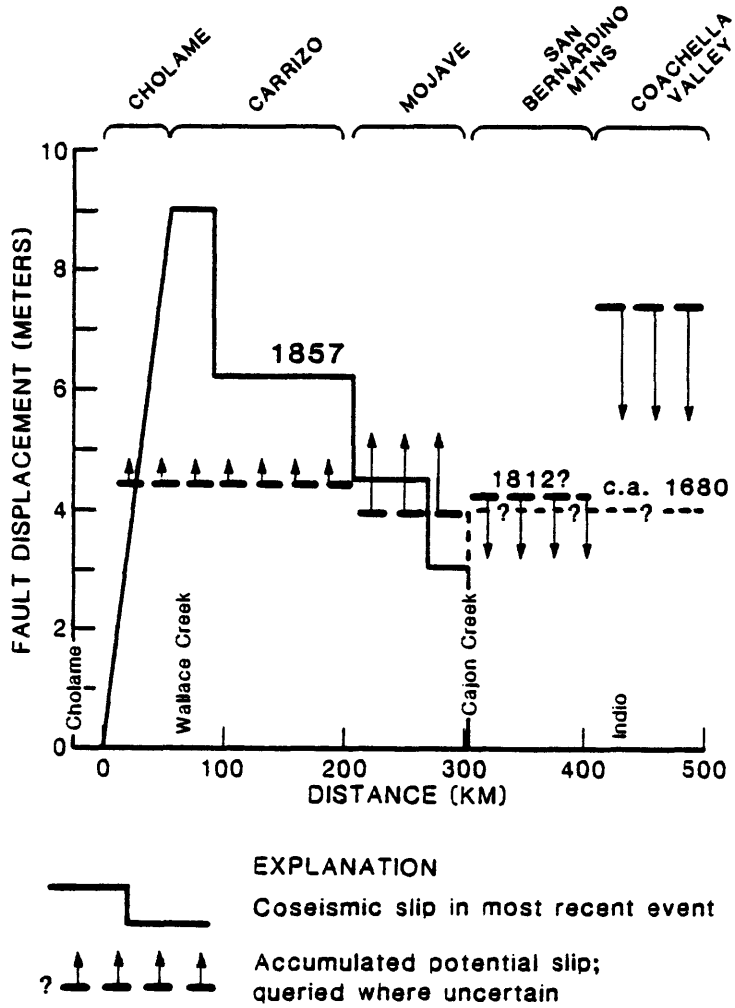

Figure 8. Slip causing historical and prehistoric earthquakes on southern San Andreas fault segments (solid lines, dashed and queried where uncertain) compared with amount of slip recovered by elastic strain accumulation since the most recent event (dashed line, arrow indicating one–standard–deviation error bar). Date indicates time of most recent event.

Central Creeping Segment. A 170-km length of the San Andreas fault in central California experiences continuous or quasi-continuous slippage, or creep [*Lisowski and Prescott*, 1981; *Brown and Wallace*, 1968]. The central 50 km of this segment is characterized by historical creep rates of 30 to 34 mm/yr. This rate of annual creep is indistinguishable from the long-term (that is, millenial) rate of slip for the fault along the Carrizo segment, to the southeast. Therefore, the Central Creeping segment of the fault does not appear to be accumulating strain for release in a large earthquake. This conclusion is supported by the geodetic observation that no strain is accumulating in the blocks adjacent to the Central Creeping segment of the fault [*Lisowski and Prescott*,

1981; *Thatcher,* 1979]. Furthermore, no historical (or prehistoric) earthquakes larger than magnitude 6 have been documented on this fault segment. In our judgment, these geologic, geodetic, and seismic observations indicate that the Central Creeping reach of the San Andreas fault is not likely to participate in the production of a large earthquake.

Parkfield Segment. The Parkfield segment comprises the 30-km length of the San Andreas fault that lies between the Central Creeping segment and the locked Cholame segment. Throughout the 20th century, surficial slip has occurred along this segment as aseismic creep and during moderate ($M = 6$) Parkfield earthquakes. The long-term hazard for magnitude 6 earthquakes on this segment has been extensively discussed by *Bakun and McEvilly* [1984] and by *Bakun and Lindh* [1985]. We have calculated from the dates of the past five Parkfield earthquakes (1881, 1901, 1922, 1934, and 1966) that the probability of a magnitude 6 Parkfield earthquake within the next 30 years is greater than 0.9. Based on a more specific recurrence model, *Bakun and Lindh* [1985] employed a probability density function with a smaller σ than that employed for this study. Consequently, their recurrence times are more narrowly defined than those given in Table 2.

Cholame Segment. The Cholame segment of the San Andreas fault extends from Cholame southeastward for about 55 km (Figure 7). It lies between the Parkfield segment of the fault, to the northwest, and the Carrizo segment, which experienced 9.5-m displacements in 1857, on the southeast.

The potential of this segment for seismic rupture in the next few decades is a matter of some debate. The controversy stems from ambiguities in the amount of slip along this segment in 1857 and in previous earthquakes. *Sieh* [1978*b*] believed, on the basis of small offset landforms, that the northwestern 20 km of this section experienced about 3.5 m of slip in 1857 and that slip in 1857 increased southeastward from 3.5 to 9.5 m along the southeastern 35 km of this segment. He also suggested that the undated event prior to 1857 was associated with about 3.5 m of slip along the northern half. Alternatively, *Lienkaemper* [1987] has suggested that the 1857 slip along the northwestern half of the segment averaged 6 ± 2 m. A group of USGS geologists visited the area in the spring of 1987, then discussed the evidence with Sieh. They concluded that the geomorphic features recorded major fault slip, but differed among themselves in their interpretations, emphasizing the ambiguous nature of the geomorphic data.

There are, however, two points of general agreement: 1) offsets associated with the 1857 earthquake are no less than 3 m and no more than 7 m along the northern half of the Cholame segment and 2) the Cholame segment represents a transition zone between the very high slip values recorded along the Carrizo segment and the small slip believed to have occurred in 1857 along the Parkfield segment.

If slip during large 1857-like earthquakes tapers from about 10 m on the southeastern end to 2 or 3 m on the northwestern end of the Cholame segment, then a time- or slip-predictable model for estimating failure of the entire segment cannot be used. A full range for model recurrence intervals, from less than 100 years for points near the northwestern end to more than 250 years for points on the southeastern end, would be calculated. If

one assumes a gradual taper in the amount of slip during large earthquakes, an obvious conclusion is that a slip deficit of northwestward-increasing magnitude exists along this segment.

Clearly the Cholame segment presents a difficult case for applying existing methods. The Working Group found no firm basis for choosing between the contentions of *Sieh* [1978b] and *Lienkaemper* [1987] regarding the true 1857 coseismic slip distribution on this segment. Regardless of the true slip distribution, its undoubted gradational nature along this 55-km-long-segment brings into question any simple calculation that depends on only a single slip value. Nonetheless, we believe the seismic hazard on this segment could well be higher than the hazard on the adjoining Carrizo segment to the southeast. For example, even using Lienkaemper's slip estimate of 6.0 ± 2.0 m as representative and applying *Sieh and Jahns* [1984] slip rate of 34 ± 1.5 mm/yr from Wallace Creek (see discussion of Carrizo segment), we find the 30-year conditional probability is 0.2. Using *Sieh's* [1978b] value of 3.5 ± 1.0 m, the probability rises to 0.5. Because we believe it is important to make a quantitative estimate of the hazard on the Cholame segment, and because the difference in interpretation between *Sieh* [1978b] and *Lienkaemper* [1987] is currently unresolved, we have made a representative calculation using a median value of 4.75 ± 2.0 m for the 1857 slip on this segment. We find that the 30-year probability in this case is then 0.3. It is assigned a level of reliability rating of *E*.

Carrizo Segment. The Carrizo segment of the San Andreas fault extends from about 145 km southeast of Cholame to about Three Points (Figure 7). In our judgment, the most reliable estimates of seismic potential for this segment derive from knowledge of the late Holocene slip rate and geomorphic evidence of slip per event. These data indicate a low seismic potential for the Carrizo segment over the next 30 years.

The northwestern 40 km of the Carrizo segment have evidence of surface dislocations of 8 to 10 m in 1857 [*Sieh*, 1978*b*]. Disruptions of small landforms along the remainder of the Carrizo segment suggest offsets were about 6 to 7 m in 1857 [*Sieh*, 1978*b*; *Davis*, 1983; *Rust*, 1983]. Throughout the Carrizo segment, the 1857 offsets appear to be similar in magnitude to offsets sustained during previous, prehistoric events [*Sieh and Jahns*, 1984].

Direct estimates of recurrence along this segment are derived from studies at Wallace Creek (Figure 7). The long-term average slip rate (34 ± 3 mm/yr)[1] and the amount of slip associated with the past three earthquakes (9.5 ± 0.5 m, 12.3 ± 1.2 m and 11.4 ± 2.5 m) are known at this site [*Sieh and Jahns*, 1984]. Slip at this site in 1857 was 2 to 3 m greater than that measured farther southeast on the Carrizo segment. As discussed by *Sieh* [1978b], at least part of this decrease may be more apparent than real, reflecting 1857 right-lateral deformation that occurred off the main San Andreas trend on this complex, multi-stranded reach of the fault. Alternatively, this difference in coseismic slip might be made up by encroachment of slip into the Carrizo segment from events occurring on the Mojave segment. In our calculations we have used the 1857 slip estimate at Wallace Creek, but somewhat increased its uncertainty, adopting a value of 9.5 ± 2.0 m. In computing

[1] 2σ error estimate.

conditional probability, we used the Wallace Creek slip rate of 34 ± 1.5 mm/yr and the 9.5 ± 2.0 m slip value to obtain a 30-year probability of 0.1.

Mojave Segment. The Mojave segment of the San Andreas fault, as defined here, extends 100 km from about Three Points to a few kilometers northwest of Cajon Creek (Figure 7). Its southeastern end corresponds to the southeastern limit of the 1857 rupture [*Sieh*, 1978*b*; *Agnew and Sieh*, 1978]. *Weldon and Matti* [1986] have proposed that this location is a good candidate for the initiation and termination of future ruptures, as well, on the basis of a contrast in the style of secondary structures and seismicity. The northwestern limit of the Mojave segment is not well-defined because the location of the northwestward increase in slip from about 3 to 7 m in 1857, upon which it is based, is poorly constrained. Seven-meter events appear to characterize events immediately northwest of Three Points [*Sieh and Jahns*, 1984; *Rust*, 1983], although small slip events (those less than about 1 m) may be undetectable using geomorphologic methods. Fault displacements of 3 to 4 m appear to characterize events farther southeast. The length of fault over which this transition occurs may be as great as 40 km [*Sieh*, 1978b]. To complicate assignment of the northwestern boundary of the Mojave segment further, *Davis* [1983] has identified three earthquake ruptures at Mill Potrero, 50 km northwest of the boundary adopted in this report. These are dated at 1435–1672,[2] 1670–1775 or 1793–1948 and 1857. The occurrence of three events at this site suggests an affinity with the Mojave segment, not the Carrizo segment. We acknowledge this inconsistency, and suggest that segment boundaries may well vary from event to event.

Information on slip rate on the Mojave segment is currently growing and thus estimates are in a state of flux. Rates from four separate studies [*Rust*, 1986; *Salyards and others*, 1987; *Schwartz and Weldon*, 1987; *Prescott and others*, 1987] range from 16 to 60 mm/yr. We believe, however, that values of 25 to 35 mm/yr are the most likely. *Salyards and others* [1987] use dated offsets for the last three slip events at Pallett Creek to obtain a value in this range averaged over the past ~500 years, and *Weldon* (unpublished data) finds a similar rate using a dated 1-million-year offset on the southeastern reach of the Mojave segment. Geodetic data permit slip rates of about the same value, although lower rates are not excluded [*Prescott and others*, 1987]. We have accordingly adopted a long-term slip rate of 30 ± 5 mm/yr for the Mojave segment.

At Pallett Creek (Figure 7) *Sieh* [1978a] identified evidence for nine large earthquakes in faulted late Holocene sediments, estimated to occur between the sixth century A.D. and 1857. He later reported evidence for three older events, as well as more data bearing upon the age and size of the latest nine [*Sieh*, 1984]. The average interval between events was

[2] We have recalculated Davis' dates using the new calibration curves from M. Stuiver's lab at the University of Washington. These dates use a lab error multiplier of 1.6, the delta^{13}C values assumed, but not measured, by the laboratory that analyzed the samples, and a confidence limit of 95%. The date Davis uses in his dissertation, 1584 ± 70, uses no lab error multiplier, assumes the same delta^{14}C values used here, and gives an error limit of 68%.

calculated to be about 145 years. The sixth and seventh events back (I and N) were found to have very small ($\leq$ 20 cm) right-lateral displacements, whereas the latest five events and the eighth event back involved 1 to 2 m of slip. The data also suggest an apparent decrease in inter-event times over the past 1000 years.

To test this possibility and narrow the range of alternative interpretations, Sieh undertook with Minze Stuiver (University of Washington) and David Brillinger (University of California, Berkeley) to date more precisely the earthquakes recorded at Pallett Creek. The table below and Figure 9 present the new dates with their 95-percent confidence limits for the most recent nine events at Pallett Creek [from *Sieh and others*, submitted].

Event	Date
Z	9 Jan 1857
X	1785 $\pm$ 32
V	1480 $\pm$ 15
T	1346 $\pm$ 17
R	1100 $\pm$ 65
N	1048 $\pm$ 33
I	997 $\pm$ 16
F	797 $\pm$ 22
D	737 $\pm$ 13
C	677 $\pm$ 13
B	> 529

Based on the analysis of tree ring data from Wrightwood, 30 km southeast of Pallett Creek, *Jacoby and others* [1987] have inferred fault slip on the San Andreas associated with the 8 December 1812 earthquake [*Toppazada and others*, 1981] and correlate it with Event X at Pallett Creek. Assuming this correlation is appropriate, the intervals calculated from these data are as follows:

Events	Interval		
Z/	131	years[3]	
X/Z	44		
V/X	332	$\pm$ 15	**Average interval:**
T/V	134	$\pm$ 23	C to Z = 131
R/T	246	$\pm$ 67	
N/R	52	$\pm$ 73	
I/N	52	$\pm$ 37	
F/I	200	$\pm$ 27	
D/F	60	$\pm$ 26	
C/D	60	$\pm$ 18	
B/C	$\geq$148	$\pm$ 31	

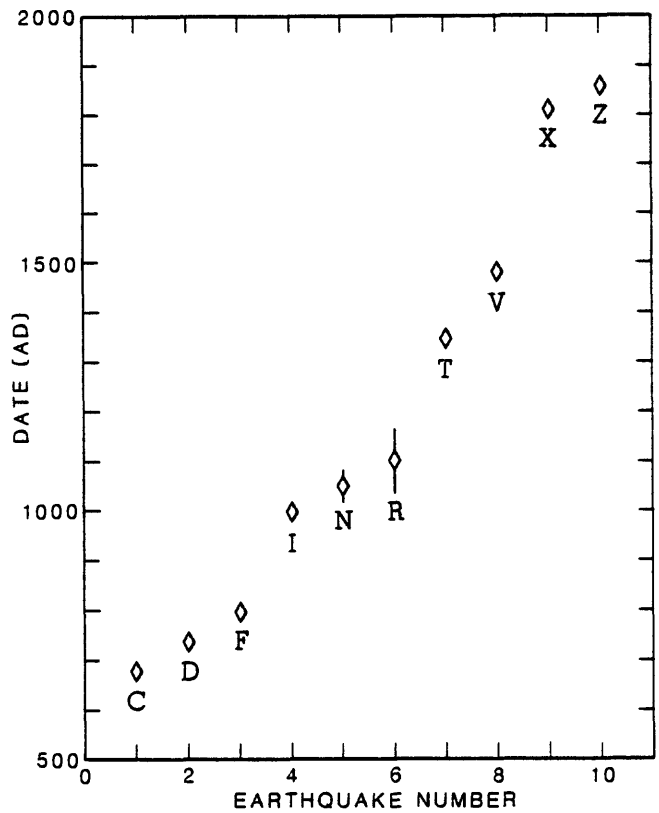

Figure 9. Dated historical and prehistoric slip events at Pallett Creek on the Mojave segment of the southern San Andreas fault. Error bars indicate 95-percent confidence intervals for each prehistoric event.

From these data and Figure 9, it is apparent that the new dates lead to significant revisions in previous conclusions concerning earthquake recurrence at Pallett Creek. First, because the revised date for Event C is later than previously reported [*Sieh*, 1984] the average recurrence interval has decreased from 145 to 131 years. Furthermore, regardless of whether or not the correlation of the 1812 earthquake with event X is correct, the interval between slip events at Pallett Creek ranges markedly from the mean value. Five of the 11 intervals are less than 100 years. Three intervals are greater than about 190 years. The new dates are precise enough to suggest that the 12 events can be partitioned into four groups or clusters. Within the clusters, intervals between earthquakes are mostly less than 100 years. The time between clusters, however, is between about 200 and 330 years.

New information also exists concerning the amount of slip in the last three slip events at Pallett Creek. Although displacement at the fault was only about 3.5 m in 1857, *Salyards*

[3]Open interval

and others [1987] have used paleomagnetic methods to reconstruct the total right-lateral warping across a 55–m–wide zone in the last three Pallett Creek events. The data suggest that total offsets per event are about 6 m [*Sieh*, personal communication]. Whether this slip should be taken as representative for the entire 100-km length of the Mojave segment is uncertain. For example, 31 values of surface fault offset in 1857 are reported by *Sieh* [1978b] for the Mojave segment and none are larger than about 4.5 m.

Although the ongoing analysis of *Salyards and others* may lead to significant changes in the assessment of 1857 slip on the Mojave segment, the Working Group felt reluctant to adopt the 6-m value as appropriate for the entire segment at this time. We have, therefore, adopted a value of 4.5 ± 1.0 m, which agrees with the maximum surface displacements reported by *Sieh* [1978*b*] and permits larger values within its error bounds.

Clearly, probabilities for large magnitude earthquakes along the Mojave segment can be calculated in a number of ways. Using our estimate of 1857 slip, 4.5 ± 1.0 m, and a slip rate of 30 ± 5 mm/yr we obtain a 30-year conditional probability of 0.3. *Sieh and others* [paper submitted to *J. Geophys. Res.*] use a Weibull function with a broad distribution to represent observed recurrence dates to obtain a 30-year conditional probability of 0.2. The broad distribution of inter–event times indicated by the new radiocarbon dates, if accepted as the complete record of characteristic earthquakes on the Mojave segment, is poorly represented by the more narrowly peaked Gaussian, lognormal, and Weibull distributions generally employed for calculations of this type and is close to being Poisson or exponential. The 30-year Poisson probability using the observed average recurrence time, T_{ave}, of 131 years yields a probability of 0.2. We regard this probability as a reasonable lower bound for this segment. For comparative purposes, the probability obtained using T_{ave} and a narrowly peaked lognormal distribution function with $\sigma = 0.21$, obtained not from the Pallett Creek data, but from the *Nishenko and Buland* [1987] analysis of worldwide recurrence data, yields a possible upper-bound 30-year probability of 0.5.

Paradoxically then, the segment for which we have the most paleoseismic data yields a long-term hazard assessment that has considerable uncertainty. Much hinges on how completely the Pallett Creek dates are representative of the history of magnitude 7 or greater events that rupture most or all of the Mojave segment. If the spread in interevent times is read literally, it suggests that, at least on this part of the San Andreas, radical revisions are necessary in prevailing ideas on the variability of earthquake recurrence intervals and the factors that regulate them. Alternatively, Pallett Creek might not be a completely representative site. For example, it could lie in a region of overlap between events rupturing predominantly northwest or southeast of the site, some of the small-displacement events could be smaller earthquakes, or some events could have been missed. In the absence of a firm quantitative basis with which to judge between these alternatives, the Working Group has chosen the direct method of calculation as the simplest to apply to this segment. Therefore, and not without some trepidation, we have used an 1857 slip value of 4.5 ± 1.0 m and a slip rate of 30 ± 5 mm/yr to calculate a 30-year conditional probability of 0.3 to the Mojave segment, with a level of reliability rating of *B*.

San Bernardino Mountains Segment. The Working Group delineated a San Bernardino Mountains segment, which comprises the fault zone between the Mojave and the Coachella Valley segments (Figure 7). The segment so defined includes two markedly different portions of the fault—the relatively simple section of the fault at the foot of the San Bernardino Mountains, north of San Bernardino, and the more complex zone of reverse, lateral, and oblique-slip faulting in the region of San Gorgonio Pass. Whether this entire segment ruptures independently or with adjacent segments is unknown. Rupture of the San Bernardino Mountains segment with the adjacent regions seems equally possible. The different scenarios have different expected magnitudes and result in somewhat different total probabilities in southern California.

It is difficult to know how to treat this segment, because we have no firm data on recurrence intervals or amount of slip per event. The fault rupture of 1857 did not include this segment of the fault, judging from the level of shaking reported by inhabitants of the San Bernardino Valley [*Agnew and Sieh*, 1978], so the current period of dormancy is greater than 131 years. Major slip on this segment of the fault could have occurred in association with the earthquake of 8 December 1812 [*Jacoby and others*, 1987, and in preparation]. Otherwise, the historical record precludes major coseismic slippage after AD 1790 [*Agnew*, 1985]. From the historical record, then, we conclude that the current period of dormancy of the San Bernardino Mountains segment is either 175 years or greater than 196 years. No creep is believed to be occurring along this segment [*Louie and others*, 1985].

In the absence of further recurrence information, we use 1812 as the tentative date of the most recent event, and available constraints on slip and slip rate to compute conditional probabilities for this segment. We use the long-term slip rate of 24 ± 3 mm/yr determined by *Weldon and Sieh* [1985] at Cajon Creek, at the northwestern end of the San Bernardino Mountains segment. These investigators suggest that offsets of about 4 m characterize the fault's most recent slippage near Cajon Creek, but we have no evidence that these values are representative of the remainder of the segment. Nonetheless, to obtain a rough quantitative estimate of hazard, assuming the segment fails independent of the adjacent segments, we used a slip value of 4 ± 2 m. Using this value and a slip rate of 24 ± 3 mm/yr, we obtain a 30-year conditional probability of 0.2, a very tentative lower bound that is assigned a level of reliability rating of *E*.

In the Discussion and Summary section that follows, we consider the possibility that this fault segment slips at the time of major earthquakes on the adjacent Mojave and Coachella Valley segments.

Coachella Valley Segment. The Coachella Valley segment, which comprises the southern 100-km of the San Andreas fault, extends from the Salton Sea on the southeast to San Gorgonio Pass on the northwest (Figure 7). This segment of the fault is characterized by a gently curving trace, steep to moderate dips, very low levels of aseismic creep [*Louie and others*, 1985], and a lack of large earthquakes during the historical period [*Agnew*, 1985].

Excavations at one locality along this segment of the fault, east of Indio, provide evidence of at least four large slip events during the period A.D. 1000 to 1700 [*Sieh*, 1986]. Their dates are 1020 ± 20, 1300 ± 90, 1450 ± 150, and 1680 ± 40. Right slip during the 1680 and 1450 events was greater than 2.0 m and greater than 3.1 m, respectively. Slip estimates are minima because lacustrine and fluvial beds at the Indio site are offset by four subparallel faults within a 50-m-wide zone and only three of the faults are preserved. At least two slip events occurred between A.D. 1000 and the 1450 event. Slip during this period was greater than 16 m. Other discrete slip events of this 700-year interval may not be detectable because deposition at the site has been sporadic. Nevertheless, these data demonstrate that this segment of the fault generates a large earthquake at least once every two to three centuries and no large earthquake appears to have occurred during the past 300 years.

At Salt Creek, near the southern terminus of the fault, where the fault has been excavated in three dimensions, slip since the early 18th century has been no more than about 110 cm [*Williams and Sieh*, 1987]. This amount is very similar to the amount of slip documented at the Indio site for a similar period. Of this amount, about 15 cm has occurred at Salt Creek since 1907. Fault slip at Salt Creek since about A.D. 1000 has amounted to only 3.5 m, a figure substantially lower than that at the Indio site [*Williams and Sieh*, 1987]. It is likely that most if not all the cumulative post-early 18th century accumulated slip represents creep. If so, the Salt Creek data are consistent with the paleoseismic record at Indio and both data sets imply an absence of large earthquakes since about 1680. No long-term fault slip rate is available at either site.

To calculate probabilities, we have assumed the inter-event times obtained at the Indio site are representative of the entire Coachella Valley segment and that the most recent event occurred in 1680±40. The average recurrence interval is then 220 ± 13 years and the 30-year conditional probability is 0.4. The low coefficient of variation for this segment ($\sigma = .30$) results from the rather tight clustering of the inter-event times obtained at the Indio site. Given the small number of events recorded there, this clustering may be more apparent than real, but the computed probabilities are not very sensitive to the assumed coefficient of variation.

San Jacinto Fault

During this century, the San Jacinto fault has produced more large earthquakes than any other in southern California, though it has no record of producing a great event comparable to those on the San Andreas fault in 1857 and 1906. Possible recurrence on this fault was first examined by *Thatcher and others* [1975], and has since been considered by *Lindh* [1983], *Sykes and Nishenko* [1984] and *Wesnousky* [1986]. At present, there are no well-constrained paleoseismic recurrence data for this fault, nor is the historical record long enough to record repeated large earthquakes for each segment. Therefore, repeat times are inferred from slip rate and amount of slip per event. In estimating the slip, we have applied the same method as that used for the Hayward fault, employing empirical fault-length/source-parameter relations to obtain approximate values of slip per event.

The selection of segments is based on recent information on slip rate, newly compiled felt-report and instrumental data on several early earthquakes [*Toppozada and others*, 1981; *Abe*, 1988], relocations of more recent events [*Sanders*, 1986], and recent results for background seismicity [*Kanamori and Magistrale*, unpublished manuscript, 1988]. The Working Group delineated five segments of the San Jacinto fault (Figure 10). During the course of our deliberations, the magnitude 6.6 Superstition Hills earthquake occurred on one of these (see discussion below). The five segments are shown in Figure 10 and the basis for their selection are listed below:

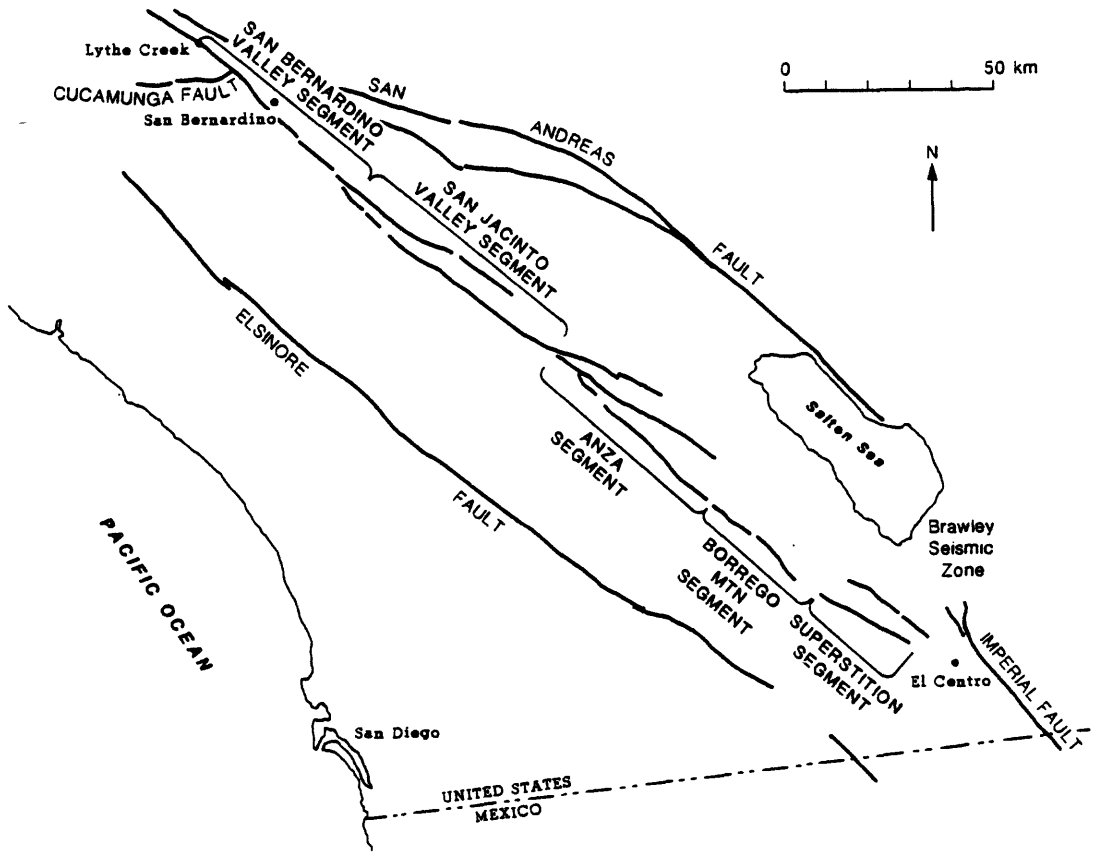

Figure 10. Segments of the San Jacinto fault zone.

Segment	Length (km)	Basis for Distinction
San Bernardino Valley	50	Lytle Creek on north to southern edge of zone characterized by shallow (>10 km) seismicity
San Jacinto Valley	65	Coincides approximately with zone in which seismicity is absent between 0–13 km depth, but which has frequent small events from 13–18 km depth. Seismicity distribution suggests uniform behavior. Possible source zone of 1918 earthquake
Anza	50	Bounded by inferred end of 1918 rupture zone on north, and north end of Borrego Mountain surface rupture on south
Borrego Mountain	50	Surface rupture zone of 1968 earthquake
Superstition	30	Superstition Hills and Superstition Mountain faults. Lies between 1968 Borrego Mountain rupture zone and 1979 Imperial fault rupture

San Bernardino Valley Segment. The San Bernardino Valley segment (Figure 10) extends approximately 50 km, from just north of the San Jacinto/Cucamonga fault intersection near Lytle Creek, to the northern end of San Jacinto Valley, where there is a notable increase in the focal depths of instrumentally recorded microearthquakes. The main fault trace in this segment is the Claremont strand, although parallel traces exist. In the absence of an historical surface faulting event, the choice of segment length is necessarily somewhat arbitrary. Seismic slip might well extend as much as 20 km beyond the Cucamunga fault intersection or terminate northwest of the point where microseismic activity deepens, so segment length could range from as little as 30 km to as much as 70 km.

Earthquake recurrence intervals and the size of a characteristic earthquake are not well-constrained. The earliest large earthquake that can be definitely located near the San Jacinto fault was that of July 1899 (Table 4), in the Lytle Creek area, though it may have

Table 4
San Jacinto Fault Zone Earthquakes

Date	Lat (°N)	Long (°W)	M_L	M_s	Moment (10^{18} N-m)	Length (km)	Slip (m)
1899/7/22	34.2	117.4	6.5	5.6	0.2		
1923/7/23	34.1	117.3	6.2		1	15	0.1
1899/12/25	33.8	117.0	6.7	6.4	4		
1918/4/21	33.8	117.0	6.8	7.0	15	50	1.2
1890/2/9	33 1/2?	116 1/4					
1980/2/25	33.52	116.55	5.0				
1937/3/25	33.47	116.42	5.9		0.3		
1969/4/28	33.34	116.35	5.8		0.5		
1954/3/19	33.30	116.18	6.2		4.4	20	0.5
1892/5/28	33 1/4?	116 1/4?					
1968/4/9	33.19	116.13	6.8		8	40	0.4
1942/10/21	33.05	116.09	6.3		9	40	0.4

been on the nearby segment of the San Andreas. *Hanks and others* [1975] assigned it a moment of 4×10^{18} N-m based on the sparse intensity data of Townley and Allen; the intensity magnitudes assigned by *Toppozada and others* [1981] suggest a local magnitude (M_L) of 6.5, giving a moment about 50 percent higher. However, *Abe* [1988] gives a surface-wave magnitude (M_s) of 5.6 from the Milne data (for only two stations, itself an indicator of small size), and this value is included in Table 5. The July 1923 ($M = 6.2$) event has been reexamined by *Sanders* [1986], who shows that the sparse instrumental and intensity data are consistent with a location on the San Jacinto fault near Loma Linda. The 1890 event could have been on this segment, but we believe the data for this event are too sparse to definitely give it the large size assigned by previous investigators. The same is true for an event in 1858 [*Toppozada and others*, 1981] that caused damage in the San Bernardino area. Trenches across the Claremont strand of the fault in San Bernardino Valley indicate at least three surface faulting events since about A.D. 250 (*Sieh*, unpublished field data), but do not define recurrence intervals.

Calculations of conditional probability for this segment are complicated by uncertainty in slip rate, amount of slip per event, and size and timing of the most recent event. *Wesnousky and others* [1987] suggest a minimum slip rate of 5.4 ± 1 mm/yr for the past 2000 years on the Claremont strand. Because of the structural complexities of this part of the zone and the proximity of the San Andreas fault, it is unclear how slip is partitioned on the different structural elements. Also, the rate of slip could be decreasing toward the end of the fault. Therefore, we have adopted a slip rate of 8 ± 3 mm/yr, which is

midway between the minimum rate of *Wesnousky and others* and the better-determined San Jacinto rate near Anza (see below), and includes both estimates within one standard deviation.

If 50 km is the true segment length, the slip versus fault-length relation suggests a characteristic slip value of 1.4 ± 0.4 m. The most recent such event on this segment could have been in 1890, although this assignment is very tentative. Using these parameters and a slip rate of 8 ± 3 mm/yr, the 30-year probability is 0.2 for an earthquake of about magnitude 7.

Given the notable uncertainties in choice of segment length, characteristic slip, and date of last event, this probability value must be regarded as very tentative. If segment length (and hence characteristic slip) were smaller or the most recent characteristic event occurred prior to 1890, then the probability would be higher. If segment length were longer, the conditional probability would be corresponding decreased. New data may well lead to substantial revision in the parameters listed in Tables 1 and 2, and this is reflected in the level of reliability rating of E shown in Table 2.

San Jacinto Valley Segment. The San Jacinto Valley segment (Figure 10) is defined on the basis of microseismic data [*Sanders*, 1986; *Kanamori and Magistrale*, unpublished manuscript, 1988] and on the inferred extent of the magnitude 6.8, 1918 earthquake. The seismicity data indicate an almost complete absence of events shallower than 13 km along an approximately 80-km-long zone of the fault. The magnitude and seismic moment of the 1918 event [*Hanks and others*, 1975] suggest a rupture length of about 50 km. Without strong evidence to choose between these two possibilities, we have assumed a median value of 65 km for the length of the San Jacinto Valley segment. The northern part of the segment contains two strands, the Claremont, which trends along the northeastern edge of San Jacinto Valley, and the Casa Loma, which is parallel. These join to form the Clark strand, which extends from the south part of San Jacinto Valley southeast to Anza.

The San Jacinto Valley has been the location of two large earthquakes, in December 1899 and April 1918. No surface rupture was observed from either event, though for the 1918 earthquake it was the subject of a specific search. As a consequence, the causative fault strands are not known with certainty. *Hanks and others* [1975] used intensity and limited instrumental data to derive a moment of 15×10^{18} N-m for the 1918 earthquake; the intensity pattern of the 1899 event was similar enough to suggest that it had the same moment. However, *Abe* [1988] has used records from undamped Milne instruments to get an M_S of 6.4 for the December 1899 event, implying the much lower moment given in Table 4.

On the Clark strand, northwest of Anza, *Rockwell and others* [1986] determined a slip rate of 9 ± 1 mm/yr for the past 9500 years. An earlier estimate by *Sharp* [1981] gave a long-term minimum rate of 8 to 12 mm/yr for the past 730,000 years. We have adopted a slip rate of 11 ± 3 mm/yr.

In the absence of other more definitive information, we have estimated characteristic slip for this segment using the empirical relation between fault length and slip. We obtain

a slip value of 1.8 ± 0.5 m. Using this estimated slip, a slip rate of 11 ± 3 mm/yr, and 70 years since the most recent event, the 30-year probability is 0.1. Once again, uncertainties in input parameters imply corresponding uncertainties in the computed probability, which is assigned a level of reliability rating of *C*.

Anza Segment. The Anza segment (Figure 10) is the region between the inferred southern end of the 1918 rupture just north of Anza and the north end of the 1968 Borrego Mountain surface rupture, a length of 50 km. It contains three fault strands: a continuation of the Clark fault, the Buck Ridge fault, and the Coyote Creek fault. An important though unresolved question is the level of activity on the different strands. It has generally been assumed that almost all the slip is on the Coyote Creek strand, for which *Sharp* [1981] estimated a slip rate of 3 to 5 mm/yr over the past 400 years, and 1 to 2 mm/yr over the past 5000 years. Sharp used these data, together with his estimation of at least 8 mm/yr farther north, to argue for a variable slip rate on the San Jacinto fault. Another possibility is that only some of the total slip for the fault zone is on this strand, with the Clark strand also having significant slip rates. *Sanders* [1986] has shown that the 1954 ($M = 6.2$) earthquake probably occurred on this strand. All this evidence suggests that although a slip rate of 11 mm/yr is valid for the whole fault zone, for any individual strand a lower rate of slip is appropriate.

Historical earthquakes on this part of the fault include the 1969 Coyote Mountain ($M = 5.8$) earthquake on the Coyote Creek fault, the 1937 ($M = 5.9$) earthquake on the Clark fault, and the 1980 Whitewash event ($M = 5.0$) on the northwest edge of the 1937 source zone. None of these is large enough to be the characteristic earthquake for a segment of this length.

There is a high degree of uncertainty in the data for calculating conditional probabilities along this part of the fault zone. There is little basis for partitioning the slip rate between the different strands of the fault, and we have used the full San Jacinto rate of 11 ± 3 mm/yr in our computations, equivalent to assuming that characteristic events on the three strands are equally spaced in time. A large earthquake in 1892 in this general region could have occurred on one of these strands, but there are no data on the timing of the most recent large event on this segment. On the basis that this is the most recent large event, assuming a slip value of 1.4 ± 0.4 m for this 50-km segment length, and applying a slip rate of 11 ± 3 mm/yr, we find a 30-year conditional probability of 0.3 with a level of reliability rating of *D*.

Borrego Mountain Segment. This segment is defined on the basis of the lateral extent of the 1968 Borrego Mountain earthquake ($M = 6.5$) surface rupture and aftershock zone on the Coyote Creek fault. This event is considered a characteristic earthquake for this part of the fault. The maximum observed surface displacement was 0.38 m, but slip at depth was probably considerably greater. Based on a geodetic estimate by *Snay and others* [1983] we have estimated slip for the 1968 event to be 0.7 ± 0.1 m for probability calculations. The slip rate is 4 ± 1 mm/yr, based on *Sharp* [1981]. These values give a mean recurrence time of 175 years. Since only 19 years have elapsed since the 1968 event, the 30-year probability

is low, calculated as less than 0.1. Because of the recency of faulting on this segment and the absence of a preceding event in the historical record, we have a high level of confidence in the hazard assessment for this segment and assign it a level of reliability rating of *B*.

Superstition Segment. The Superstition segment (Figure 10) contains more than one active strand, including the parallel Superstition Hills and Superstition Mountain faults, each about 30 km long. The Superstition Hills fault experienced minor slip in response to nearby earthquakes in 1951, 1968, 1979, and 1981, and has undergone episodic creep at other times. No slip rate data or paleoseismic recurrence times are available nor (when the Working Group first met) was the time of the last earthquake known. A preliminary assessment (using a slip rate of 4 mm/yr, slip of 0.6 m, and time of last earthquake in 1892) gave a conditional probability of 0.2 for a magnitude 6 1/2 earthquake on this segment in the next 30 years. At a later meeting on 23 November, the Working Group discussed this segment further and decided that the level of information was so poor for this segment (poorer than for any other) that no estimate of conditional probability could be justified.

Ironically, 30 km of the Superstition Hills fault ruptured in a magnitude 6.6 event the next day. While validating our choice of segment, this experience well illustrates a major problem in attempting probabilistic long-term earthquake prediction for active faults in California. While knowledge of particular segments may often be less than would justify a quantitative assessment, our ignorance does not imply the fault is less hazardous. The 1987 Superstition Hills earthquake shows that many fault segments deserve close attention, whether or not quantitative hazard assessments can be narrowly constrained (or even established) by the data available.

We believe the current level of hazard on the Superstition segment is low. However, because of the absence of reliable slip rate information we have not formally estimated conditional probabilities for the next 30 years.

Imperial Fault

The Imperial fault (Figure 10) spans the border between the United States and Mexico in the Imperial Valley and has produced at least two and possibly five earthquakes greater than magnitude 6 in this century [*Johnson and Hill*, 1982]. The two unquestionable events are also the largest (1940, $M = 7.1$ and 1979, $M = 6.6$). Both were associated with surface rupture along the Imperial fault. Although the pattern and amplitude of the surface displacements were quite similar over the northern 25 km of the fault break [*Sharp*, 1982], slippage at seismogenic depths were considerably greater in the 1940 earthquake [*Snay and others*, 1982; *Thatcher, Zhang, and Snay*; work in progress] and 1940 fault slip extended about 35 km farther southeast of the termination of the 1979 rupture. On the northern ~30 km of the Imperial fault, seismic slip at depth was 1.8 to 2.2 m in 1940 and about 0.8 m in 1979. Slippage on the southernmost 30 km of the 1940 rupture was considerably greater, 4 to 8 m.

The long-term slip rate on the Imperial fault is not well-determined. Surface creep rates are as much as 8 mm/yr on the northern 30 km of the fault [*Louie and others*, 1985]

but surface creep dies out at the southern end of the 1979 rupture and is not observed farther southeast. Geodetic survey results for the interval 1941–78 suggest rates of 30 to 40 mm/yr, but it is not clear to what degree this may be contaminated by aftereffects of the 1940 earthquake [*Thatcher, Zhang, and Snay*, work in progress]. We have assumed a value of 30 ± 5 mm/yr.

Although the average fault slip in the 1979 earthquake was about 0.8 m, two independent studies using strong motion data from that event show that the detailed slip distribution was highly non-uniform [*Archuletta*, 1984; *Hartzell and Heaton*, 1983]. These studies show a zone of ~10 km extent on the south-central reach of the 1979 rupture that experienced coseismic slip averaging about 1.2 m. This coseismic slip may be more crucial in controlling the recurrence characteristics of the 30-km-long 1979 rupture than is the average slip on the segment. For the northern 35 km of the Imperial fault, we have used the peak slip in the 1979 earthquake, 120 ± 40 cm, and a slip rate of 30 ± 5 mm/yr to compute the 30-year probability for a 1979-type event. We obtain a value of 0.5 and assign it a level of reliability rating of *C*.

Other Faults of the Southern San Andreas Fault System

Brawley Fault and Brawley Seismic Zone. The Brawley fault, a north-trending splay from the Imperial fault, experienced surface fault displacement at the time of the 1940 and 1979 earthquakes on the Imperial fault [*Sharp*, 1982], as well as during a sequence of smaller earthquakes in 1975. Indeed, the region of the Brawley fault has been associated with several intense sequences of small earthquakes, leading to the informal designation, "Brawley seismic zone" (Figure 10). This zone extends northward beyond the termination of the mapped Brawley fault, and beneath the Salton Sea, where it terminates upon intersecting the San Andreas fault near Bombay Beach [*Johnson and Hill*, 1982]. Clearly, the Brawley seismic zone plays an important role in the tectonic connection of the Imperial and San Andreas faults. However, it is believed the zone does not represent a throughgoing fault, but rather a series of en echelon steps [*Hill and others*, 1975; *Johnson and Hadley*, 1976]. The Brawley seismic zone was the source of the 1981 Westmoreland earthquake ($M = 5.7$), and may have been responsible for other earthquakes in the magnitude 6 range, the locations of which are not well determined by the information available. Again, the seismic hazard associated with the possible occurrence of earthquakes in the magnitude 6 range seems high in this region [*Wesson and Nicholson*, 1988], but there is currently no evidence to suggest that the Brawley seismic zone could generate a larger earthquake, unless it were also associated with rupture of the Imperial fault to the south or the San Andreas fault to the north. For the purposes of this report, there is little basis for making probabilistic assessments of long-term potential for earthquakes of magnitude 7 or greater.

Elsinore Fault. Recent geologic estimates of slip on the Elsinore fault give rates of about 5 mm/yr for the region between Lake Elsinore and the international border [*Millman and Rockwell*, 1985; *Vaughn and Rockwell*, 1986]. However, geodetic measurements [*King and Savage*, 1983] do not show any strain accumulation across this fault. In view of this

discrepancy it seems especially imprudent to make any probabilistic calculations. Only one earthquake can be definitely associated with this fault, a magnitude 6 event on 6 May 1910. Farther south, the earthquake of 9 February 1892 was probably associated with this fault zone, though it is disputed whether it was on the Agua Caliente section north of the border or on the Laguna Salada fault to the south. If we assume that the geometry of the fault is such that it produces characteristic earthquakes with a slip of 1 m, the recurrence time would be about 200 years. This means that, in the absence of other data, the most recent earthquake could have occurred as recently as 100 years ago, implying a low probability of a repeat event in the next 30 years, or (say) 300 years ago, implying a high probability. For the purposes of this report, there is little basis for making probabilistic assessments of long-term potential for earthquakes of magnitude 7 or greater.

DISCUSSION AND SUMMARY

This study has used the historical seismic record, paleoseismic evidence, and results from geology, geodesy and seismology to assess the seismic potential of the major strands of the San Andreas fault system in California. Use of these data sources in a probabilistic framework has permitted us to refine and quantify what a more casual survey of historical large earthquakes suggests – that seismic hazard is generally high where large or great earthquakes have not occurred for ~100 years or more, and is generally low or moderate elsewhere. For example, we find that the 30-year seismic potential for magnitude 7 or greater events is low over most of the 450-km-long rupture of the great 1906 earthquake on the northern San Andreas. In contrast, the hazard is moderate or high on much of the 500-km-length of the southern San Andreas, where the most recent large earthquake was in 1857, on the segment of the Hayward fault believed to have slipped in an event of about magnitude 7 in 1836, and over those segments of the San Jacinto fault that have not sustained significant seismic slip in this century.

On several segments of the San Andreas system, even qualitative hazard assessments require more information than is supplied by the historical seismic record alone. For example, rupture on the Carrizo segment of the south–central San Andreas has not occurred for 131 years; however, slip per event and slip rate information provided by paleoseismic investigations indicate a recurrence interval for this segment of about 300 years. Again, although no historical earthquakes larger than magnitude 6 have occurred on the Central Creeping segment of the San Andreas, the absence of geodetically measurable elastic strain accumulation along this reach of the fault indicates that the seismic potential for magnitude 7 earthquakes along this segment is at least extremely low and is probably negligible.

The limitations imposed on our study deserve note and it should be emphasized that new work will doubtless alter our values of conditional probability. Chief among the limitations of our analysis is the paucity of relevant data, especially recurrence and slip rate information on several crucial fault segments. Even where recurrence time data are available, as at Pallett Creek on the Mojave segment, ambiguities in interpretation are evident, pointing to the importance of obtaining dates for prehistoric events at multiple sites on the same fault segment. One of the central assumptions of our analysis is that either inter-event times for a segment cluster around a single mean value, or that amount of slip, time of the last event, and the long-term fault slip rate can be used directly to forecast the time of the next major shock (time-predictable model). Clearly more and better site-specific data on inter-event times, amount of slip, and slip rate from the San Andreas system will refine our probabilistic calculations, and new data from California and elsewhere will test current hypotheses concerning the degree of regularity of earthquake recurrence and the factors governing it.

Although the limitations of this study deserve emphasis, we nonetheless believe our principal conclusions concerning total likelihood of occurrence of one or more earthquakes in the San Francisco Bay Area and the two regions in southern California, aggregated from the individual probabilities are robust (Table 3). This is because the method of

computing the total probabilities, and expected characteristics of revisions of the individual probabilities both tend to make the total probabilities more stable than the individual probability values. The change in an individual probability is always greater than the change it can cause in total probability as given by equation (6). This is illustrated by the removal of the San Bernardino Mountains segment (30-year probability of 0.2) from the total probability for the southern San Andreas fault in Table 3, which reduces the total probability from 0.7 to 0.6 for the 30-year interval. Additionally, as new data become available, we expect that some revisions of the individual probabilities will likely be both higher and lower, and hence the changes will tend to cancel when aggregated into the total probability for a region. This can be expected for improvements of those data that are not systematically biased, or where changes reflect a conservation of the overall slip or moment budget of a region. An example of the latter would be the adjustment of the boundary between segments, which would tend to increase the recurrence time on the segment that is lengthened and decrease the recurrence time on the segment that is shortened. Other changes of the data, especially regional adjustment of average slip rates, will systematically change probabilities of all fault segments affected.

The probability of a magnitude 7 earthquake originating on at least one of the San Francisco Bay area fault segments is considered to be moderate to high, with a 5-year probability of 0.1 and a 30-year probability of 0.5. Three fault segments have been identified in the San Francisco Bay area that are believed to be capable of generating large earthquakes. The San Francisco Peninsula segment of the San Andreas fault, which last slipped in the great 1906 earthquake, was found to present a low to moderate hazard for a magnitude 7 event, a less than 0.1 probability over the next 5 years and 0.2 probability over 30 years. The Hayward fault was the site of two magnitude 7 earthquakes in the 19th century and those fault segments have comparable 30-year probabilities (0.2 each). The North Coast segment of the San Andreas fault, which extends north from San Francisco, is judged to represent a low probability for a magnitude 7 earthquake in the next 30 years.

The probability of magnitude $7\frac{1}{2}$ to 8 earthquakes is moderate or high throughout the 300-km length of the southern San Andreas from Tejon Pass to the Salton Sea. The hazard appears greatest for the Coachella Valley segment, where a major earthquake has not occurred since about 1680. The Mojave segment has a nearly comparable level of hazard. Great uncertainty surrounds the San Bernardino Mountains segment, which may have slipped in 1812. The total probabilities for a magnitude $7\frac{1}{2}$ or greater earthquake on at least one of these segments is 0.2 and 0.7 for 5- and 30-year intervals, respectively.

If the San Bernardino Mountains segment does not slip independently, but ruptures along with earthquakes on either the Mojave or Coachella Valley segments, then larger earthquakes associated with fault ruptures 200 km long and magnitudes of about 7.8 will result. Slip of all three of the segments in a single earthquake would result in an earthquake of about magnitude 8. We judge that it is equally possible that the San Bernardino Mountains segment will slip independent of the adjacent segments, or that slip on either the Mojave or Coachella Valley segments will cause slip on the San Bernardino Mountains segment. For the latter case, the total probability of a major earthquake along the southern San Andreas fault is that obtained from aggregating the probabilities for the

the Mojave and Coachella Valley segments as given in Table 3, and is 0.6 for the next 30 years. Other scenarios are also plausible, such as rupture from the San Bernardino Mountains segment into the Mojave or Coachella Valley segments. The estimation of the effects of ground motion for each postulated earthquake is beyond the scope of this report. One approach that lends itself to the use of multiple scenarios for the southern California region appears in *Evernden and Thompson* [1985].

Less is known about the characteristics of the five identified segments of the San Jacinto fault; three of the segments, San Bernardino Valley, San Jacinto Valley and Anza, pose at least a moderate hazard of producing a magnitude 7 earthquake in the next 30 years. The two remaining segments, Borrego Mountain and Superstition, pose a low hazard for the coming 30 years because of recent earthquakes on those segments. The Borrego Mountain segment experienced an earthquake in 1968. During the writing of this report, the November 24, 1987 (M_s = 6.6) Superstition Hills earthquake occurred on a segment we previously identified and tentatively assigned a 30-year probability of 0.2. The total probability for the San Jacinto fault for events in the magnitude range of 6 1/2 to 7 is 0.1 and 0.5 for 5- and 30-year intervals, respectively.

Other faults in California may generate large earthquakes, but were judged not to have sufficient data to apply the methods employed in this report. Consequently, we remind the reader that the total probability for a large earthquake originating on all faults in a region could substantially exceed those calculated for the San Andreas fault system.

REFERENCES

Abe, K., 1988, Magnitudes and origin times from Milne seismograph data: earthquakes in China and California, in Lee, W.H.K., Meyers, H. and Shimazaki, M., editors, Historical Seismograms and Earthquakes of the World: *Academic Press*, London, p. 37–50.

Agnew, D., 1985, Evidence on large southern California earthquakes from historical records: unpublished manuscript.

Agnew, D. and Sieh, K., 1978, A documentary study of the felt effects of the great California earthquake of 1857: *Seismol Soc. America Bull.*, **68**, p. 1717–1729.

Algermissen, S.T., Perkins, D.M., Thenhaus, P.C., Hanson, S.H., and Bender, B.L., 1982, Probablistic estimates of maximum acceleration and velocity in rock in the contiguous United States: *U.S. Geol. Surv. Open-File Rep. 82-1033*, 99 p.

Archuletta, R.J., 1984, A faulting model for the 1979 Imperial Valley earthquake: *J. Geophys. Res.*, **89**, p. 4559–4585.

Bakun, W.H., and Lindh, A.G., 1985, The Parkfield, California earthquake prediction experiment: *Science*, **229**, p. 619–624.

Bakun, W.H., and McEvilly, T.V., 1984, Recurrence models and the Parkfield, California, earthquakes: *J. Geophys. Res.*, **89**, p. 3051–3058.

Bonilla, M.G., Mark, R.K., and Lienkaemper, J.J., 1984, Statistical relations among earthquake magnitude, surface rupture length, and surface fault displacement: *Bull. Seismol. Soc. Am.*, **74**, p. 2379–2411.

Brown, R.D., and Wallace, R.E., 1968, Current and historic fault movement along the San Andreas fault between Paicines and Camp Dix, California, in Dickinson, W.R. and A. Grantz, editors, Proceedings of conference on geologic problems of San Andreas fault system: *Stanford Univ. Pubs. Geol. Sci.*, **11**, p. 22–41.

Clark, M.M., Harms, K.K., Lienkaemper, J.J., Harwood, D.S., Lajoie, K.R., Matti, J.C., Perkins, J.A., Rymer, M.J., Sarna-Wojcicki, A.M., Sharp, R.V., Sims, J.D., Tinsky, J.C., and Ziony, J.I., 1984, Preliminary slip-rate table for late Quaternary faults of California: *U.S. Geol. Surv. Open-File Rept 84-106*, 12 p.

Cummings, J.C., 1983, The Woodside Facies, Santa Clara Formation and late Quaternary slip on the San Andreas fault, San Mateo County, California (abstract): 58th Annual Meeting Program and Abstracts, **82**, *American Association of Petroleum Geologists*, Tulsa, Okla.

Danforth, J.C., 1987, Earthquake insurance; Problems and options: Committee on Commerce, Science, and Transportation, U.S. Senate. U.S. Government Printing Office, 61 p.

Davis, T.L., 1983, Late Cenozoic structure and tectonic history of the western "big bend" of the San Andreas fault and adjacent San Emigdio Mountains: unpublished Ph.D. dissertation, University of California, Santa Barbara, 580 p.

Dieterich, J.H., 1984, Earthquake mechanisms and modeling: *Annual Review of Earth and Planetary Science*, **2**, p. 275–301.

Evernden, J.F. and Thompson, J.M., 1985, Predicting seismic intensities, in Evaluating earthquake hazards in the Los Angeles Region - An Earth–science Perspective, J.I. Ziony, ed., *U.S. Geological Survey Prof. Paper 1360*, p. 151–202.

FEMA, 1980, An assessment of the consequences and preparations for a catastrophic California earthquake; findings and actions taken: *Federal Emergency Management Agency*, 59 p.

Hagiwara, Y., 1974, Probability of earthquake occurrence as obtained from a Weibull distribution analysis of crustal strain: *Tectonophysics*, **23**, p. 313–318.

Hall, N.T., 1984, Holocene history of the San Andreas fault between Crystal Springs Reservoir and San Andreas Dam, San Mateo County: *Bull. Seismol. Soc. Am.*, **74**, p. 281–299.

Hanks, T.C., Hileman, J.A., and Thatcher, W., 1975, Seismic moments of the larger earthquakes of the southern California region: *Geol. Soc. Am. Bull.*, **86**, p. 1131–1139.

Hanks, T.C., and Kanamori, H., 1979, A moment-magnitude scale: *J. Geophys. Res.*, **84**, p. 2348–2350.

Hartzell, S.H., and Heaton, T.H., 1983, Inversion of strong ground motion and teleseismic waveform data for the fault rupture history of the 1979 Imperial Valley, California, earthquake: *Bull. Seism. Soc. Am.*, **73**, p. 1553–1583.

Hill, D.P., Mowinckel, P., and Peake, L.G., 1975, Earthquakes, active faults, and geothermal areas in the Imperial Valley, California: *Science*, **188**, p. 1306–1308.

Jacoby, G.C., Sheppard, P.R., and Sieh, K.E., 1987, Was the 8 December 1812 California earthquake produced by the San Andreas fault? Evidence from trees near Wrightwood (abstract): Seismol. Soc. Am., Proc. 82nd Annual Mtg., *Seismol. Res. Lett.*, **58**, no. 1, p. 14.

Johnson, C.E., and Hadley, D.M., 1976, Tectonic implications of the Brawley earthquake swarm, Imperial Valley, California, January 1975: *Bull. Seismol. Soc. Am.*, 66, p. 1133–1144.

Johnson, C.E., and Hill, D.P., 1982, Seismicity of the Imperial Valley, in The Imperial Valley, California, Earthquake of October 15, 1979: *U.S. Geol. Survey Prof. Paper 1254*, p. 15–24.

Kanamori, H., and Anderson, D.L., 1975, Theoretical basis of some empirical relations in seismology: *Bull. Seismol. Soc. Am.*, 65, p. 1073–1096.

King, N.E. and Savage, J.C., 1983, Strain rate profile across the Elsinore, San Jacinto, and the San Andreas faults near Palm Springs, California: *Geophys. Res. Lett.*, **10**, p. 55–57.

Lawson, A.C. ed., 1908, The California earthquake of April 18, 1906: Report of the State Earthquake Investigation Commission, *Carnegie Inst. of Washington*, Washington, D.C., 447 p.

Lienkaemper, J., 1987, 1857 Slip on the San Andreas fault southeast of Cholame, CA: *EOS, Trans. Am. Geophys. Union*, **68**, p. 1506.

Lindh, A.G., 1983, Preliminary assessment of long-term probabilities for large earthquakes along selected segments of the San Andreas fault system in California: *U.S. Geol. Surv. Open-File Rep. 83-63*, p. 1–5.

Lisowski, M., and Prescott, W., 1981, Short-range distance measurements along the San Andreas fault system in central California, 1975 to 1979: *Seismol. Soc. America Bull.*, **71**, p. 1607–1624.

Louderback, G.D., 1947, Central California earthquakes of the 1830's: *Bull. Seis. Soc. Amer.*, **37**, p. 33–74.

Louie, J.N., Allen, C.R., Johnson, D.C., Haase, P.C. and Cohn, S.N., 1985, Fault slip in southern California, *Bull. Seismol. Soc. Am.*, **75**, p. 811–833.

Millman, D.E., and Rockwell, T.K., 1985, Lateral offset of mid- and late-Quaternary deposits along the northern Elsinore fault, southern California: Abstracts with Programs, *Geol. Soc. of Am.*, **17**, no. 6, p. 370.

Nason, R.D., 1971, Investigation of fault creep slippage in northern and central California: University of California, San Diego, Ph.D. dissertation.

Nishenko, S.P., 1985, Seismic potential for large and great interplate earthquakes along the Chilean and southern Peruvian margins of South America: A quantitative reappraisal, *Jour. Geophys. Res.*, **90**, p. 3589–3615.

Nishenko, S.P., 1989, Earthquake Hazard and prediction: *Van Norstand Rheinholt Encyclopedia of Geophysics*, in press.

Nishenko, S.P., and Buland, R., 1987, A generic recurrence interval distribution for earthquake forecasting: *Bull. Seismo. Soc. Am.*, **77**, p. 1382–1399.

Prescott, W.H., Lisowski, M., and Savage, J.C., 1981, Geodetic measurement of crustal deformation on the San Andreas, Hayward, and Calaveras faults near San Francisco, California: *Jour. Geophys. Res.*, **86**, p. 10853–10869.

Prescott, W.H., and Lisowski, M., 1982, Deformation along the Hayward and Calaveras faults: Steady aseismic slip or strain accumulation, in Proceedings, Conference on Earthquake Hazards in the Eastern San Francisco Bay Area: *Special Publication 62, Calif. Div. Mines and Geol.*, Sacramento, p. 231–238.

Prescott, W.H., and Lisowski, M., 1983, Strain accumulation along the San Andreas fault system east of San Francisco Bay, California: *Tectonophysics*, **97**, p. 41–56.

Prescott, W.H., and Yu, S.-B., 1986, Geodetic measurement of horizontal deformation in the northern San Francisco Bay region, California: *Jour. Geophys. Res.*, **91**, p. 7475–7484.

Prescott, W.H., Lisowski, M. and Savage, J.C., 1987, Velocity field along the San Andreas fault in southern California: *EOS, Trans. Am. Geophys. Union*, **68**, p. 1506.

Rockwell, T., Merrifield, P.M., and Loughman, C.C., 1986, Holocene activity of the San Jacinto in the Anza seismic gap, southern California: Abstracts with Programs, *Geol. Soc. Am.*, **18**, no. 2, p. 177.

Rust, D.J., 1983, Trenching studies of the San Andreas fault bordering western Antelope Valley, southern California: in Summaries of Technical Reports, National Earthquake Hazard Reduction Program, *U.S. Geol. Survey*, XVI, p. 70–71.

Rust, D.J., 1986, Neotectonic behavior of the San Andreas fault zone in the Big Bend: Abstracts with Programs, *Geol. Soc. Am.*, **18**, no. 2, p. 179.

Salyards, S.L, Sieh, K.E., and Kirschvink, J.L., 1987, Paleomagnetic measurement of dextral warping during the past three large earthquakes at Pallett Creek, southern California: Abstracts with Programs, *Geol. Soc. Am.* (in press).

Sanders, C.O., 1986, Seismotectonics of the San Jacinto fault zone and the Anza seismic gap, unpublished Ph.D. dissertation, California Institute of Technology, Pasadena, 143 pp.

Scholz, C.H., 1982, Scaling laws for large earthquakes: consequences for physical models: *Bull. Seismol. Soc. Am.*, **72**, p. 1–14.

Scholz, C.H., 1985, The Black Mountain asperity: seismic hazard of the southern San Francisco peninsula, California: *Geophys. Res. Lett.*, **12**, p. 717–719.

Schwartz, D.P. and Weldon, R.J., 1987, San Andreas slip rates: preliminary results from the 96 St. site near Littlerock, CA: Abstracts with Programs, *Geol. Soc. Am.*, **19**, no. 6, p. 448.

Schwartz, D.P., and Coppersmith, K.J., 1984, Fault behavior and characteristic earthquakes, examples from the Wasatch and San Andreas fault zones: *Jour. Geophys. Res.*, **89**, p. 5681–5698.

Sharp, R.V., 1981, Variable rates of late Quaternary strike-slip on the San Jacinto fault zone, southern California: *J. Geophys. Res.*, **86**, p. 1754–1762.

Sharp, R.V., 1982, Comparison of 1979 Surface faulting with earlier displacements in the Imperial Valley, in The Imperial Valley, California, Earthquake of October 15, 1979: *U.S. Geol. Survey Prof. Paper 1254*, p. 1213–1222.

Shimizaki, K., and Nakata, T., 1980, Time-predictable recurrence model for large earthquakes: *Geophys. Res. Lett.*, **7**, p. 279–282.

Sieh, K., 1978a, Pre-historic large earthquakes produced by slip on the San Andreas fault at Pallett Creek, California: *Jour. Geophys. Res.*, **83**, p. 3907–3939.

Sieh, K., 1978b, Slip along the San Andreas fault associated with the great 1857 earthquake: *Seismol. Soc. America Bull.*, **68**, p. 1421–1428.

Sieh, K., 1984, Lateral offsets and revised dates of large earthquakes at Pallett Creek, California: *Jour. Geophys. Res.*, **89**, p. 7641–7670.

Sieh, K., 1986, Slip rate across the San Andreas fault and prehistoric earthquakes at Indio, California: in *EOS, Trans. Am. Geophy. Union*, **67**, p. 1200.

Sieh, K., and Jahns, R.H., 1984, Holocene activity of the San Andreas fault at Wallace Creek, California: *Geol. Soc. America Bull.*, **95**, p. 883–896.

Snay, R.A., Cline, M.W., and Timmerman, E.L., 1982, Horizontal deformation in the Imperial Valley, California, between 1934 and 1980: *Jour. Geophys. Res.*, **87**, p. 3959–3968.

Snay, R.A., Cline, M.W., and Timmerman, E.L., 1983, Regional deformation of the earth model for the San Diego region, California: *J. Geophys. Res.*, **88**, p. 5009–5024.

Sykes, L.R. and Nishenko, S.P., 1984, Probabilities of occurrence of large plate rupturing earthquakes for the San Andreas, San Jacinto, and Imperial faults, California, 1983–2003: *Jour. Geophys. Res.*, **89**, p. 5905–5927.

Sykes, L.R., and Quittmeyer, R.C., 1981, Repeat times of great earthquakes along simple plate boundaries, in Simpson, D.W., and Richards, P.G., editors, *Earthquake Prediction, An International Review, Maurice Ewing Ser.* **4**, Am. Geophys. Union, Washington, D.C., p. 217–247.

Thatcher, W., 1979, Systematic inversion of geodetic data in central California: *J. Geophys. Res.*, **84**, p. 2283–2295.

Thatcher, W., Hileman, J.A., and Hanks, T.C., 1975, Seismic slip distribution along the San Jacinto fault zone, southern California, and its implications: *Bull. Geol. Soc. Am.*, **86**, p. 1140–1146.

Thatcher, W., and Lisowski, M., 1987a, Long-term seismic potential of the San Andreas fault southeast of San Francisco: *Jour. Geophys. Res.*, **92**, p. 4771–4784.

Thatcher, W., and Lisowski, M., 1987b, 1906 earthquake slip on the San Andreas fault in offshore northwestern California: *EOS, Trans. Am. Geophys. Union*, **68**, p. 1507.

Toppozada, T.R., Reel, C.R., and Parke, D.L., 1981, Preparation of isoseismal maps and summaries of reported effects for pre-1900 California earthquakes: *Calif. Div. Mines Geol. Open-File Rep. 81-11*, Sacramento, 182 p.

Vaughan, P., and Rockwell, T., 1986, Alluvial stratigraphy and neotectonics of the Elsinore fault zone at Aqua Tibia Mountain, southern California: in Ehlig, P.L., compiler, Neotectonics and faulting in southern California, Guidebook and Volume, Cordilleran Section, *Geol. Soc. Am.*, p. 177–191.

Weldon, R., and Matti, J., 1986, Geologic evidence for segmentation of the southern San Andreas fault: *EOS, Trans. Am. Geophys. Union*, **67**, p. 905–906.

Weldon, R.J., and Sieh, K.E., 1985, Holocene rate of slip and tentative recurrence interval for large earthquakes on the San Andreas fault in Cajon Pass, southern California: *Geol. Soc. Am. Bull.*, **96**, p. 793–812.

Wesnousky, S.G., 1986, Earthquakes, Quaternary faults, and seismic hazard in California: *Jour. Geophys. Res.*, **91**, p. 12587–12631.

Wesnousky, S., Scholz, C.H., Shimizaki, K., and Matsuda, T., 1983, Earthquake frequency distribution and the mechanics of faulting: *Jour. Geophys. Res.*, **88**, p. 9331–9340.

Wesnousky, S.G., Prentice, C.S., and Sieh, K.E., 1987, Fault slip rate determination on the northern segment of the San Jacinto fault, San Bernardino, California: *EOS, Trans. Am. Geophys. Union*, **68**, p. 1506.

Wesson, R.L., and Nicholson, C., 1988, Intermediate-term, preearthquake phenomena in California, 1975–1986, and preliminary forecast of seismicity for the next decade: *PAGEOPH*, in press.

Williams, P.L., and Sieh, K.E., 1987, Decreasing activity of the southernmost San Andreas fault during the past millennium: Abstracts with Programs, *Geol. Soc. Am.* (in press).

APPENDIX

EARTHQUAKE DATA

We present here in greater detail the types of data that form the basis for the probability calculations. This is provided as brief background for evaluating the various factors and limitations affecting the results of this study. The basic data and their applicability to the forecasting problem are summarized below.

Data for Earthquake Parameters

Source	Time	Location	Slip	Fault Length	Available After
Local Seismometers	E	G–E	G	E	1920–30
Distant Seismometers	E	F–G	G	F	1900
Felt Reports	E	P–F	P–F	P	1850
Paleoseismic Evidence	P	E	P–G	F	~1000
Surface Displacement	NA	E	G	G	1906*
Geodetic Surveys	NA	**	†	†	1906*

E: excellent; G: good; F: fair; P: poor; NA: not applicable
* only available in some cases
** not generally used to define this
† G for the product of these two

Lists of times, places, and sizes of earthquakes—referred to as historical seismicity data—are basic to probabilistic forecasts. It is important to note that the type of forecast considered in this study requires accurate information about a relatively few large earthquakes (the characteristic earthquakes of each segment). The sources of data include instrumental records, direct observations of slip, felt reports, paleoseismic evidence, and empirical relationships.

Instrumental Records

Recordings by seismometers provide the most accurate seismicity data possible, with complete coverage and exact timing. A network of seismometers can give a very precise location for an earthquake, though unless the network is well distributed, this location may be too inaccurate to allow an earthquake to be associated with a particular fault. Some of the best available estimates of coseismic slip are obtained from analysis of seismograms (as interpreted using models of the earthquake source), though even with many high quality records such estimates can vary by a factor of 2.

Seismic recording began in California in 1887, with the establishment of stations at Berkeley and Mount Hamilton. The northern California network remained largely concentrated in the San Francisco Bay area until the late 1950's. Seismic recording in southern California began in the 1920's, and a sparse network covering much of the area was operating by 1932. Neither network could provide highly accurate locations until the major densifications that accompanied the use of telemetry (around 1970); however, many of these earlier locations can be improved by using more recent recordings to determine station corrections.

Estimates of earthquake size (whether as magnitude or seismic moment) require that the available seismographs be well-calibrated. For local recording in California, this is generally true after about 1930, when a number of Wood-Anderson instruments were in operation. Unfortunately, these recordings were liable to be driven offscale by large earthquakes, whose sizes must then be estimated using records from more distant stations. Few distant stations were adequately calibrated prior to the establishment of the World Wide Seismograph Network in the early 1960's. Before 1930, instrumental data on earthquake size is very sparse, though still valuable when available. There are no instrumental data for California earthquakes prior to 1887.

Direct Observations of Slip

Though seismograms provide the best evidence that an earthquake has occurred, they can only provide indirect estimates of the basic earthquake source properties (that is, rupture dimensions and amount of displacement). For those earthquakes large enough to cause surface breakage, direct estimates of displacement and the length of faulting can be obtained from field observations. Such data were first collected following the 1906 earthquake, and are available for most large California earthquakes since that time. Although these estimates may seem ideal, they are not without possible error. Measurements along a surface break are representative of slip within a narrow zone (<100 m) at the surface. It is quite possible that deeper coseismic slip might propagate only partially to the surface and might be reflected as deformation over a much broader zone than just at a fault trace. Hence, surface slip measurements could easily underestimate the extent and amount of displacement at depth.

Precise geodetic measurements in the area surrounding the earthquake provide one of the best measures of earthquake size. Note, however, that unless these geodetic measurements are made just before and after the earthquake, they will capture more than just the coseismic deformation. Unfortunately, adequate geodetic data are available for only a few California earthquakes, and along the fault zones considered in this study, only the data collected for the 1906 earthquake add to our knowledge of the event.

Felt Reports

Prior to the deployment of seismograph networks, the best information on earthquake occurrence comes from reports of how strongly events were felt in different places. For

California, systematic collection and appraisal of these reports began after the 1906 earthquake, and so precede the establishment of seismograph recording by only a few decades. Earlier reports are largely dependent on newspaper articles, which can be vague and biased. The most serious problem in using these data comes from the very uneven distribution of population in both space and time. Even now, large parts of southern California are too sparsely inhabited to provide many felt reports for some earthquakes.

Felt reports can provide information about the time of an earthquake, and sometimes the general location, but they cannot give an accurate location (unless there is associated surface faulting). It is possible to estimate the size of an earthquake from the area shaken at a given intensity level, provided enough reports are available. The relation between felt area and earthquake size, however, is much less precise than an instrumental determination of earthquake size, and area shaken at a given intensity can have uncertainties of at least a factor of 3.

The systematic reporting of natural events in California starts with the beginning of journalism (and large population increases) in 1850. Before this time, the record of felt earthquakes is extremely incomplete, and the few reported events can be given only for very general locations. During this earlier period, it is quite possible that some large (magnitude 7) events would not have been reported, at least in any form that would make them recognizable as such. In the desert areas of southern California, including most of the San Jacinto fault, moderate (magnitude 6.5 to 7.0) events could have been missed as late as 1890.

Paleoseismic Evidence

Prior to the time of written records in California (1769), the seismic record depends on the relatively new discipline of paleoseismology. Paleoseismology is the study of prehistoric earthquakes as revealed primarily in the geologic record. Techniques involve analysis of strata that have been offset by faults at the time of earthquakes, commonly as exposed in fine-scale excavations. In addition, prehistoric earthquakes can be identified by the analysis of the shapes of fault scarps, or of uplifted marine or river terraces. The ^{14}C method is probably the most commonly used of more than two dozen dating techniques for determining the age of prehistoric events.

Although offset beds are indicative of slip on the faults that cut them, these are single-point observations, and the correlation of offsets from site to site and their association with specific earthquakes can be problematic. These geographic problems are coupled with potentially significant temporal errors, partially from uncertainties in the dating procedure and partially from the nature of the procedure, which can only provide bounds as to the time of faulting. In some cases, precise dates can be determined using tree-rings from trees near the fault, but the time span of this technique is limited.

Estimates of coseismic slip can be made not only at the sites discussed above, but at many other places where linear features (such as a streambed) are crossed by the fault. Even if no dateable material is present, the sequence of disruptions can be determined, and

by correlating these sequences from site to site, a picture of fault slip can be established. As yet, it is impossible to distinguish disruptions due to fault creep from sudden displacements due to faulting. However, the presence of liquification features is diagnostic of earthquake shaking.

Empirical Relationships

As noted previously, the inadequacy of our seismicity data often requires us to estimate earthquake recurrence time using the ratio of slip rate to coseismic displacement. For many of the segments discussed in this report, we have no data on the amount of slip during the last event, so it has to be estimated from empirical relations that relate the amount of slip to magnitude and fault length. Rates of fault slip are determined for individual faults using geologic or geodetic data.

Geologic estimates of slip rate are based on taking a dateable feature with some amount of displacement, and dividing the amount by the age. Both quantities are subject to the usual measurement errors. Geologic estimates can also include fault creep, but an even greater source of uncertainty is that such slip rates represent long-term geologic averages whose relevance to the present day rates of fault slip are uncertain in many cases.

Accurate estimates of current rates of fault slip must rely on high-precision geodetic data. These have been routinely collected only in the last decade, but, where available, can provide a fairly reliable estimate of recent strain accumulation. The major uncertainties in using these data arise from the spatial averaging needed to get reliable results. In structurally complex areas, such averaging can render unclear the specific source of the observed motions.